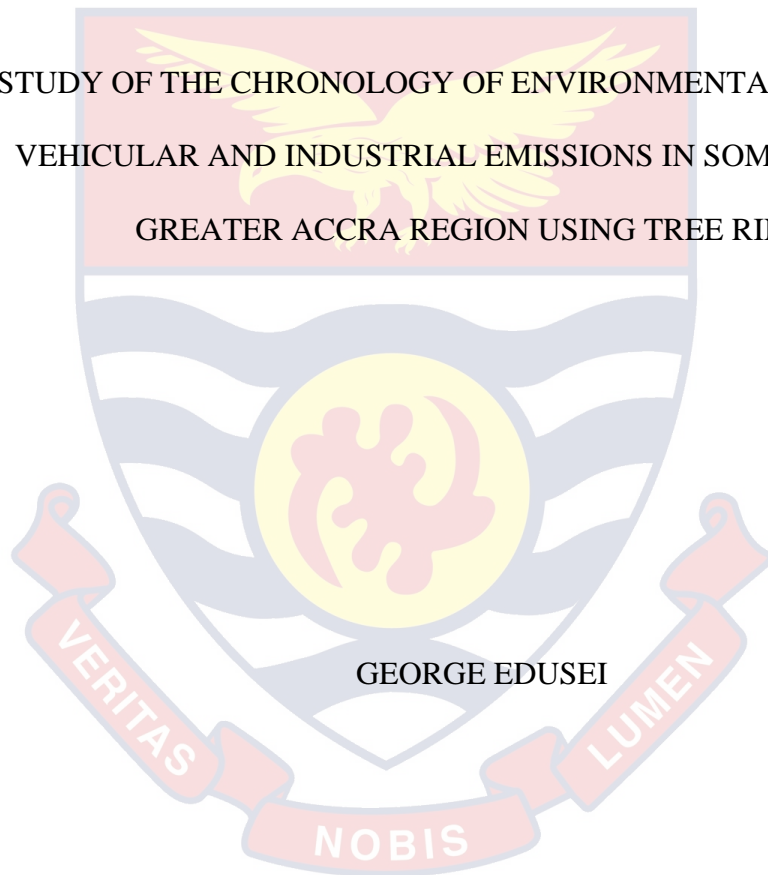UNIVERSITY OF CAPE COAST

STUDY OF THE CHRONOLOGY OF ENVIRONMENTAL IMPACT OF

VEHICULAR AND INDUSTRIAL EMISSIONS IN SOME PARTS OF

GREATER ACCRA REGION USING TREE RINGS

GEORGE EDUSEI

2020

© George Edusei

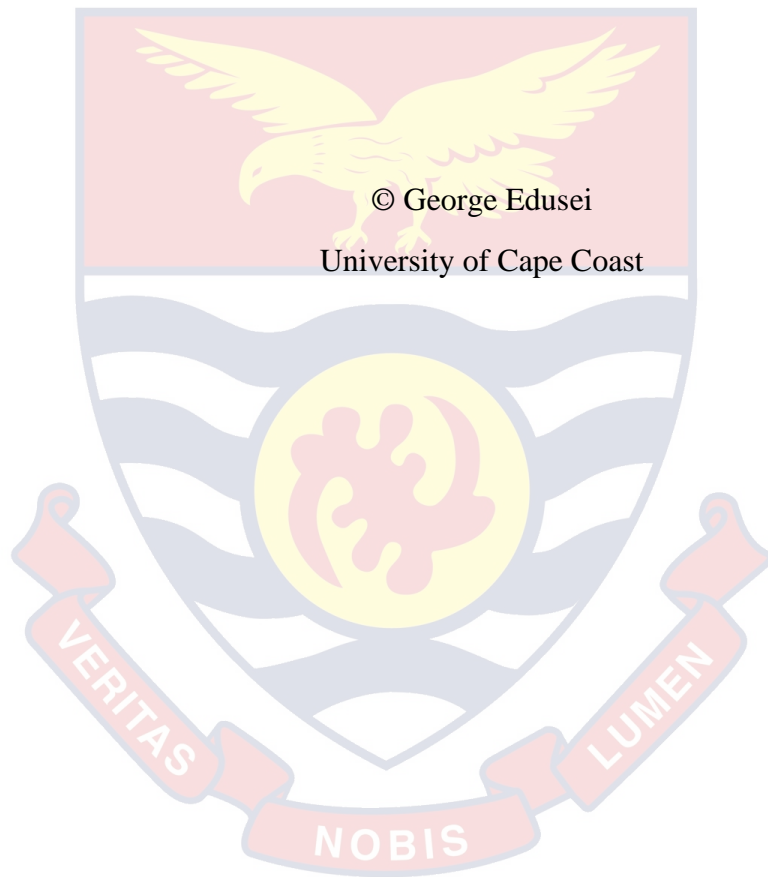University of Cape Coast

UNIVERSITY OF CAPE COAST

STUDY OF THE CHRONOLOGY OF ENVIRONMENTAL IMPACT OF

VEHICULAR AND INDUSTRIAL EMISSIONS IN SOME PARTS OF
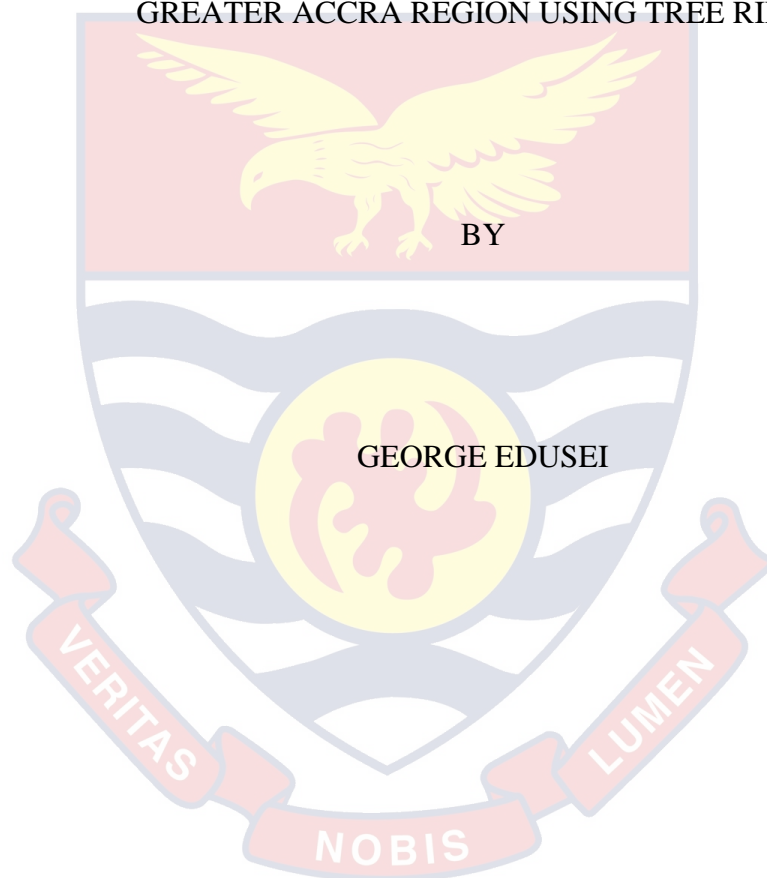
GREATER ACCRA REGION USING TREE RINGS

BY

GEORGE EDUSEI

Thesis Submitted to the Department of Physics of the School of Physical
Sciences, College of Agriculture and Natural Sciences, University of Cape
Coast in partial fulfilment of the requirement for award of Doctor of
Philosophy degree in Physics

OCTOBER 2020

DECLARATION

Candidate's Declaration

I hereby declare that this thesis is the result of my own original research and that

no part of it has been presented for another degree in this university or elsewhere.

Candidate's Signature ……………………………. Date………………
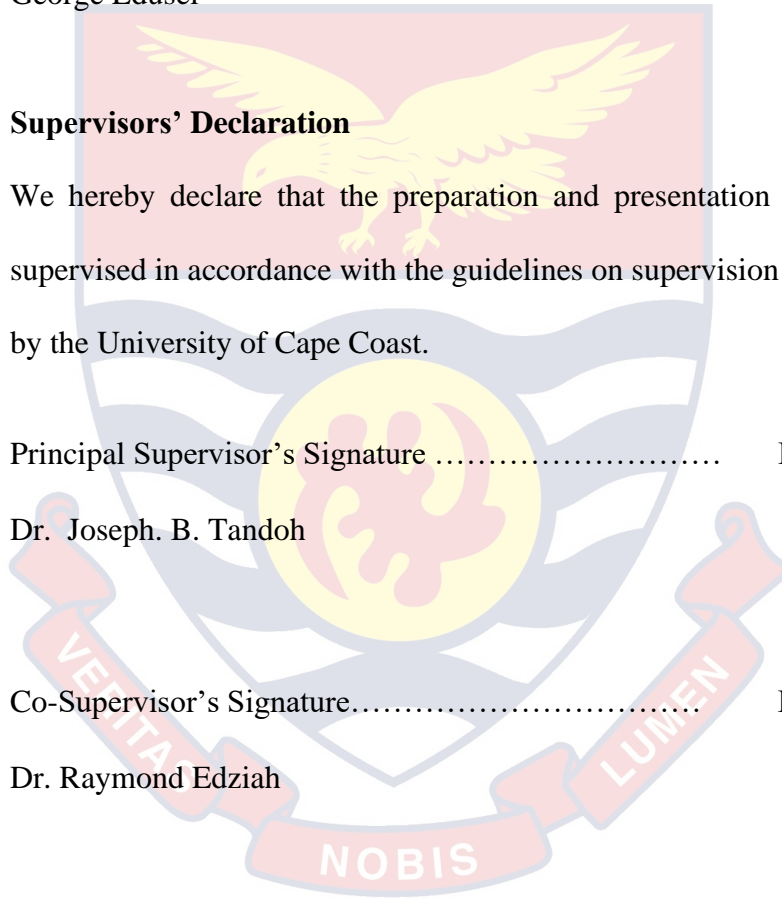
George Edusei

Supervisors' Declaration

We hereby declare that the preparation and presentation of the thesis were

supervised in accordance with the guidelines on supervision of thesis laid down

by the University of Cape Coast.

Principal Supervisor's Signature ……………………… Date……………...

Dr. Joseph. B. Tandoh

Co-Supervisor's Signature…………………………. Date………………

Dr. Raymond Edziah

ABSTRACT

This study determined the heavy metals pollution chronologies from vehicular and industrial emissions in the atmosphere using tree-rings as bio-indicators. Haatso atomic road and Tema Industrial area in the Greater Accra Region over the years have been the major hot spots for vehicular and industrial pollution respectively. Swietenia mahagoni (Mahogany) tree which is over 50 years in age was chosen for this study because it produces annual growth rings which is vital for the reconstruction of past climates. Tree ring counting method was used to determine the ages of both trees, at the various locations; Haatso Atomic road (1957-2018) and Tema Industrial Area (1968 - 2018). Energy Dispersive X-ray Fluorescence (EDXRF) was utilized to determine the presence and concentration of the following heavy metals (Cu, Mn, Zn, Pb, Cd, Fe and Ni) in the tree rings sampled. Concentration of Cu, Mn, Zn, Pb, Cd, Fe and Ni at the two sampling sites ranged from (1.92—9.84mg/kg), (2.58 – 5.49 mg/kg), (5.37 – 15.78mg/kg), (0.12—0.60 mg/kg), (0.01—0.09 mg/kg) (11.21—90.13 mg/kg) and (0.10 – 0.99 mg/kg) respectively. Surprisingly an increasing trend in concentration was observed for (Cd, Fe and Mn) with levels higher than the WHO guideline for heavy metals in the plant. The concentration of Cu, Zn, Pb, and Ni at both sampling sites were below WHO maximum limit by a factor of 1.2. Statistical analysis performed on the data from both sites revealed a strong positive correlation (0.85) between growth rings width of tree sampled from Haatso-Atomic road and that of the Tema Industrial area. It was observed that wet seasons correlate with high growth rate of trees while low precipitation seasons correspond to low or no growth rate of trees.

KEY WORDS

Vehicular emission

Industrial emission

EDXRF techniques

Annual tree rings

Heavy metals

Air pollution

ACKNOWLEDGEMENTS

I would like to express my sincere gratitude to my supervisors Dr. Joseph Tandoh and Dr. Raymond Edziah for their continuous help, numerous suggestions and guidance to make this research work possible.

Moreover, I am very thankful to Dr. George Banini, Dr. Owiredu Gyampo, and Dr. Hyacinthe Ahiamadjie for their assistance in the course of this work.

Finally, I am grateful to my adorable wife Gladys Agyapomah Edusei, my lovely daughter Akosua Edusei, Christian Subaar, Shemmira Yunus and all my friends and loved ones who helped in diverse ways to make this work a success.
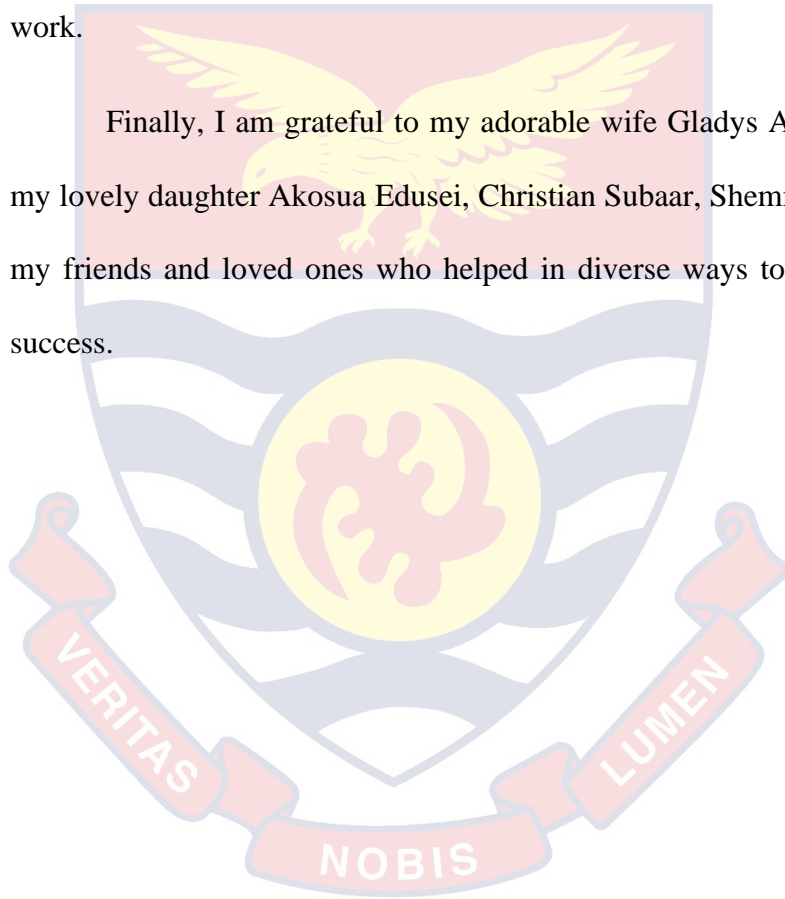
DEDICATION

To my late father Mr. Philip Kofi Edusei and Mr. Yaw Nsuo Brobbey

TABLE OF CONTENTS

CHAPTER THREE: RESEARCH METHODS

CHAPTER FOUR: RESULTS AND DISCUSSION

LIST OF TABLES

LIST OF FIGURES

LIST OF ACRONYMS

APM	Atmospheric Particulate Matter
CA	Cluster Analysis
EC	Elemental Carbon
EF	Enrichment Factor
EDXRF	Energy Dispersive X-ray Fluorescence
EPA	Environmental Protection Agency
GAEC	Ghana Atomic Energy Commission
IAEA	International Atomic Energy Agency
PIXE	Particle Induced X-ray Emission
PM	Particulate Matter
PCA	Principal Component Analysis
PMF	Positive Matrix Factorization
SSA	Sub-Saharan Africa
UNEP	United Nations Environment Programme
USAID	United States Agency for International Development
USEPA	United States Environmental Protection Agency
WHO	World Health Organization
XRF	X-ray Fluorescence

CHAPTER ONE

INTRODUCTION

Background to the Study

In an urban environment heavy metal pollutant are released from many different anthropogenic sources, such as, vehicles, industries, building construction or renovation, waste incineration, agriculture (fertilizers and pesticides etc) Celik et al., 1995; Wajid et al., 2008; Popescu, 2011; Tanvir et al., 2017). Road transport activities over the past decades have increased as a result of the world's economic growth and improved human welfare (Siyan et al., 2015; Elena et al., 2018). Consequently, the rise of road transport activities causes high levels of pollutant emissions which impact negatively on the environment, especially farmlands, pastures, rivers and residences along heavy vehicular traffic areas and major highways. (Oliva & Espinoza, 2007; Lee et al., 2010).

Motor vehicles introduce a number of toxic metals into the atmosphere which are later deposited on roadside, increasing Pb, Zn, Cr, Ni, S, Fe, Cd, Cu and Mn concentrations in road dust and vegetation adjacent the roadside (Lough et al., 2005). Pb comes from the exhaust of vehicles which is attributed to the addition of lead alkyl as an antiknock additive to gasoline to raise octane number of fuel. Copper emissions are also as a result of the wear of brake linings (Vecchi et al., 2007; Abu-Allaban et al., 2003; Garg et al., 2000). At high levels or concentration, these metals can cause serious health risks to humans. However, exposure to high concentrations of airborne manganese for prolonged periods of time can produce adverse health effects affecting primarily the nervous system leading to slower visual reaction time, poorer hand steadiness, and impaired eye-hand coordination (Aboh, 2000).

1

Monitoring of air pollution using bioindicators is emerging as a potentially effective and more economical alternative in performing direct ambient air measurements. Most air pollution studies in Ghana are based on atmospheric aerosols collected on particulate matter filters (Aboh et al., 2012; Benjamin & Ayatulai-Abdul, 2018). This is an active method that gives an idea of trace-element in atmospheric pollution only during the sampling time (Kathie et al., 2010). It requires long-term sampling at a large number of sampling sites. The measurements require sophisticated technical equipment which are generally expensive. In Ghana, it is difficult to use air samplers in remote areas due to lack of electricity. The usefulness of bioindicators such as mosses, tree rings and lichens in determining trace- and heavy-metal concentrations in different geographical areas has been discussed and demonstrated in several studies (Markert, 2003; Tan et al., 2005; Padmo et al., 2003).

Mosses and lichens are used because they more readily reflect local changes in heavy-metal deposition and they are also better accumulation indicators (Palmieri et al., 2016). A disadvantage of using mosses and lichens as passive samplers is that their growing range is limited. Mosses and lichens generally do not grow in dry areas, making it hard to perform studies across different types of biomes or at all sites where air pollution monitoring is needed (e.g., at industrial sites) (Szczepaniak & Biziuk, 2003).

Even though mosses and lichens have shown good indication as bio-indicators for air pollution, they cannot be used as proxies for historical environmental information and also they cannot be used for reconstructing climate back in time. A number of studies have shown the ability of trees to take up and incorporate pollutants into their annual growth rings (Nabais et al., 2001; Speer, 2010). Indeed, tree-rings have been used to provide annual records of

2

pollution over decades, tracing pollutants on a spatial and temporal scale in relation to their sources (Cocozza et al., 2016; Danek et al., 2015; Odabasi et al., 2015).   In this study the interest is in vehicular and industrial emission chronology recorded in tree rings over the past fifty (50) years at Haatso-Atomic and Tema industrial area in the Greater Accra region. Tree-ring based climate reconstructions are important in developing and validating climate models for understanding past climate conditions. Therefore, in this study concentrations of heavy metal in tree-rings would be examined to reflect heavy metals pollution variations. Also in this study growth rates of trees would be related to rainfall patterns around the sampling points. This phenomenon is summarized in Figure 1, where growth rates are higher in wet seasons than in dry seasons.
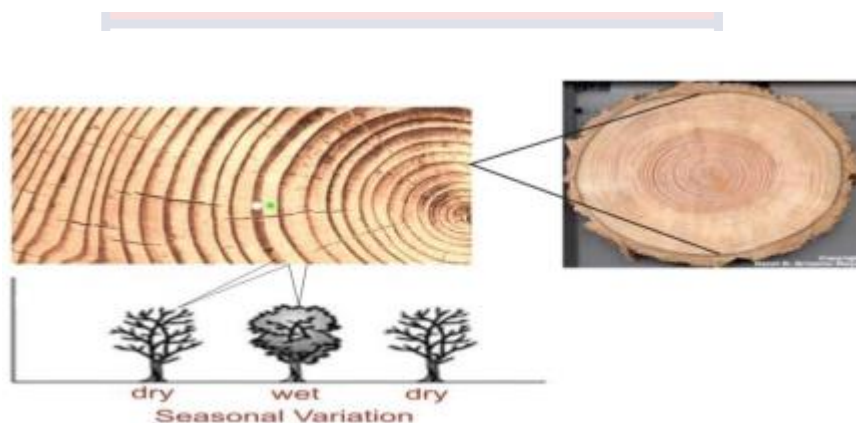
Figure 1: Tree Rings Growth with Respect to Seasonal Variation (Yorke and Omotosho, 2010).

Statement of the Problem

Motor vehicles and industries have been known to contribute to poor air quality (Kadiyala & Kumar, 2013). They emit different pollutants such as carbon monoxide, sulphur, particulate matter (PM) and ozone. With the increasing urbanization in developing countries like Ghana, there is an associated increase in population resulting in increase in the use of vehicles both for private and

3

public use. Traffic congestion on our roads and industrial activities in Greater Accra have significantly increased over the past 10 years, causing an increased pollutant emission from vehicles and industries which degrades the ambient air quality (Schrank & Lomax, 2007). Poor air quality has harmful effects on human health, particularly the respiratory and cardiovascular systems (Chang et al., 2016). Recent studies have shown excess morbidity and mortality for drivers, commuter and individuals living near major roadways and industries (Batterman et al., 2013). In Ghana, studies carried out by researchers (Nerquaye-Tetteh, 2009 & Dionisio et al, 2010), revealed high concentrations (219.20 - 236.00 $\mu g/m^3$) of heavy metal (Zn, Ni, Cu and Mn) in the city of Accra especially at roadside locations. Work done by (Safo-Adu et al., 2014) on heavy metals (Zn, Ni, Cu and Mn) along the Accra-Tema Highway also revealed $86.97\mu g/m^3$ and $17.82\mu g/m^3$ concentrations exceeding WHO standards

The elemental concentrations in tree-rings of pine along the past ten years from vehicles in Central Mexico was assessed. Elemental analyses were done with Particle Induced X-ray Emission (PIXE) spectrometry. The results showed the concentration in tree-rings corresponding to elements S, Ni, Cu, and Zn (German et al., 2004). In Ghana studies looked at atmospheric aerosols collected on PM filters which gives an idea of trace-element atmospheric pollution only during the sampling time. Presently, our understanding of past trends of air pollution impacts from traffic congestion on roads and industries is very limited. Therefore, this study seeks to use tree rings as bio-indicators to investigate atmospheric pollution of heavy metals which would give historical environmental information and reconstructing climate back in time (1957 to 2018).

Research Objectives

To determine heavy metals pollution chronologies from vehicular and industrial emissions in the atmosphere using tree-rings dating about 50 years as bio-indicators.

Specific Objectives

1. To determine heavy metal composition in tree-rings.

2. To correlate the levels of atmospheric pollution with tree biomass growth rate using ring widths

3. To correlate tree-ring growth to climatic conditions such as rainfall and drought.

Significance of the Study

Climate change is due to both natural and anthropogenic causes. Among the several natural "sentinels" of climate change, trees potentially represent excellent indicators for reconstructing the changing climatic conditions in the recent and remote past and for monitoring the impacts of the current global warming and the related environmental conditions. Motor vehicles and pollutants from industries have been known to contribute immensely to poor air quality (Krzyzanowski & Cohen, 2008). Different pollutants that negatively impact air quality have different capacities of toxic activity on humans and the ecosystem. The disease burden on developing nations such as Ghana results in high levels of mortality (WHO, 2016).

Chemical elements and pollutants derived from human activities can mask the climatic signal but, at the same time, trees become precious collectors of data that could be used for multidisciplinary research. Therefore, this study

5

would provide information that would improve or enhance national quality guidelines on emissions especially on remediation activities. Published results from this study will give insight into the trend of heavy metal pollution chronology. Based on the data to be acquired from this study, future predictive pollution trend of heavy metals levels models could be developed.

Scope of the Research

This research only focuses on the Tema heavy industrial area and the Haasto-Atomic road in the Greater Accra Region of Ghana, with the purpose to determine heavy metal pollution chronologies from industrial and vehicular emissions with time resolution recorded in tree-rings dating about 50 years. In addition, correlation of atmospheric pollution with tree growth rate using rings widths will be studied. Correlation of tree-ring growth to climatic conditions such as rainfall and drought would also be investigated.

Organization of the Study

This research work is organized into five chapters. Chapter one deals with the introduction of the thesis, highlight and background of the thesis. Statement of the problem of the research, objective and scope, significance of the study as well as the structure of the thesis. Chapter two reviews the literature used in this study and taking reviews of previous works done in line with industrial and vehicular emissions chronologies in the heavy industrial and heavy traffic areas. Chapter three presents the materials and the methodology to be adopted in carrying out this research. Chapter four deals with the results that have been generated with an in depth presentation and discussion of the results and its implications. Chapter five gives inferences leading to conclusions reached and recommendation for possible areas for future research work.

CHAPTER TWO

LITERATURE REVIEW

Introduction

This review covers overview of atmospheric pollution in Ghana, particulate matter in vehicular traffic, health effects of selected heavy metals, biomonitoring of air pollution using mosses, lichen and tree rings, other studies related to the heavy metal pollution, interactions of x-ray with matter energy, dispersive x-ray fluorescence (EDXRF) spectrometry and enrichment factor.

Overview of Atmospheric Pollution in Ghana

In Ghana, and most of the other sub-Saharan Africa (SSA) countries, there is absence of regular and systematic air quality-monitoring for air quality assessment. As a result, there is lack of data on the concentrations as well as the characteristics of atmospheric particulate matter. There have been routine monitoring programs in Accra by the Environmental Protection Agency of Ghana (EPA-Ghana) to measure only PM_{10}. However, there is no systematic record of $PM_{2.5}$ concentrations in Accra, partly because air quality standard for $PM_{2.5}$ has not been established in Ghana (Hughes, 2014)

The EPA-Ghana between 2005 and 2008 collaborated with the United States Agency for International Development (USAID), the United States Environmental Protection Agency (USEPA) and the United Nations Environment Programme (UNEP) to set up an urban air quality monitoring network in Accra. The objective of the project was to accurately characterize the importance and nature of air pollution problems in Accra and to make recommendations for the development of air quality management strategy for Ghana (Hughes, 2014). Results from the study revealed that vehicular exhaust

7

emissions, emissions from industrial sources, commercial activities and wind-blown dust were the major contributors to the air quality measured at the monitoring sites (Figure 2).

Figure 2: (a) Vehicular Exhaust Emissions and (b) Industrial Emission in Greater Accra, Ghana. (Air Pollution in Ghana, Accra Ghana/23 February, 2019. https://www. atcmask.com)

Road traffic congestion is becoming the fastest source of pollution in many major urban centers in SSA (Jones et al., 2016). Motorization in the Greater Accra Region is high by African standards, at 90 vehicles per 1,000 populations, as compared to 20-30 for Nairobi, and Addis Ababa (GEF, 2007). This is partially because of the high number of taxis, public mini bus transport and motorcycles used for commercial services. There has been a significant growth in the imported vehicles into the country (Hughes, 2014).

Particulate Matter in Vehicular Traffic

Transportation is the single principal source of air pollution in urban areas (Agyemang et al., 2007). The UNEP estimates that about 90% of urban air pollution in speedily growing cities in developing countries is as a product of

vehicle emissions (UNEP, 2010). The rapidly growing numbers of motor vehicles in urban cities of developing countries are posing serious risk to the health of the population. Traffic-related particles from vehicles fall mainly into the submicron or fine mode range. They are able to penetrate deep into the respiratory tract, especially into the alveolar regions of the lung. In most SSA urban cities, the vehicle emissions problem tends to be dominated by emissions from the high number of old and poorly maintained motor vehicles without catalytic converters, and the use of poor-quality fuel (Kojima & Lovei, 2001).

Moreover, the increasing numbers of used cars and poor road networks have led to traffic congestion in most African cities. Almost 70% of the vehicles imported into Ghana are second-hand vehicles (GAM, 2019). Traffic congestion can cause vehicular emissions to increase appreciably, which could lead to high human exposures to traffic-related pollutants (Vardoulakis et al., 2003). Traffic congestion in urban areas hampers economic productivity, damages people's health, and degrades the quality of their lives.

Exhaust emissions from both diesel and gasoline fueled vehicles have been identified as a major source of primary and secondary anthropogenic aerosols in urban cities. Road-traffic emissions in urban areas come from a number of sources, which include vehicle exhaust or tailpipe emissions (both fuel and lubricating oil combustion) and contributions from non-exhaust vehicle-related particles emissions (Rogge et al., 1993; Kupiainen, 2007). A study by (Kam et al, 2012) in developed countries showed that exhaust emissions contributed predominantly to fine PM and non-exhaust emissions contributed mainly to the coarse PM.

Vehicle exhaust emissions consist of particles formed in the internal combustion engines as product of incomplete combustion. The particles derived from vehicle exhaust emission are primarily composed of elemental carbon and organic carbon. Exhaust or tailpipe emissions depend on the type and age of the engine, the type of fuel and the lubricant used, and the configuration of the exhaust system (Ondrrcek et al., 2011). Heavy metals that have often been associated with vehicular emissions include Cu, Zn, Pb, Br, Fe, Ca, Cr, and Ba (Wahlin et al., 2006; Thorpe & Harrison, 2008).

Non-exhaust emissions from on-road vehicles consist of non-combustion particles from tires and brake wear, road surface abrasion and re-suspension of road dust induced by the vehicle generated turbulence (Thorpe and Harrison, 2008). Abrasion of brake linings and tires and re-suspended road dust, for example, release to the atmosphere particles with traces of elements such as strontium (Sr), copper (Cu), molybdenum (Mo), barium (Ba), cadmium (Cd), chromium (Cr), manganese (Mn) and iron (Fe) (EC, 2004).

Re-suspension of road dust depends on a number of factors – road surface, humidity, intensity of traffic and wind speed. Substantial contributions of Al, Si, K, Ca, Ti, Mn, Fe, Zn and Sr, mostly in the coarse particle fraction, are apportioned to the road/tyres source. Non-exhaust particles can contribute significantly, to overall particulate emissions from the transport sector. However, the scarcity of data in developing countries on non-exhaust emissions makes it difficult to quantify its impact on the overall ambient concentrations (Kupiainen, 2007).

Health Effects of Selected Heavy Metals

Heavy metals have been categorized amongst the most hazardous groups of man-made pollutants in the environment. This is due to their toxic and persistent nature in the environment. Although they occur naturally in the environment, their levels may be highly elevated as a result of anthropogenic undertakings such as mining, combustion of fossil fuels, metal smelting amongst others. Certain metals like Pb, Cd and Cu are known to be hazardous contaminants which are capable of accumulating in the human body for relatively long periods of time (Leili et al., 2008).

The existence of particulate metals in the ambient air at elevated levels may have adverse health effects on humans. Pb, for example at elevated levels may induce neurological and hematological effects. It may also interfere with metabolism and bio-accumulate in living tissues (Razos & Christides, 2010).

Effect of Zinc

Zinc is a vital element for living tissues since it is involved in biochemical processes which are required for physiological functions like sexual function and normal immune function. Traditionally, zinc has been considered as a non- toxic element but current studies reveal that free ionic zinc could eradicate neurons, gill and other types of cell. High dose and short term exposures are usually the cause of acute zinc effects. This however depends on the point of contact. At a lower level of zinc exposure coupled with a prolonged period of time, chronic somatic effects may arise. Also, intense inhalation of industrial fumes containing zinc oxide in humans can induce a disease condition known as metal fume fever. Symptoms of this metal fume fever include chills, fever, chest pains and cough (Nriagu, 2007).

Effects of Copper

At low concentrations, copper, a reddish metal may be found in the soil, water, rocks, sediments and air. Its concentrations in the ambient air ranges from a few nanograms to about 200 ng/m3. Copper may find its way into the environment via emissions such as mining of copper, burning of fossil fuels and from natural sources like windblown dust (ATSDR, 2004). Copper is an essential element for living organisms including humans at low levels of intake. It is necessary for the development and functioning of the central nervous system and the brain. Deficiencies in copper may affect the development of the brain as well as abnormalities in brain function (Opazo et al., 2014). At much higher levels, toxic effects such as headaches, dizziness, and irritation of the nose, mouth, and eyes may occur. Copper intakes at extremely high doses may also result in kidney and liver injury, and eventually lead to premature death (ATSDR, 2004).

Effects of Cadmium

Cadmium is often found in the earth's crust in association with other metal ores like lead and zinc. In the atmosphere, it exists in the form of particulates and sometimes vapor (ATSDR, 2012). The health effects of cadmium are well documented. The USEPA classify it as being carcinogenic to humans. Prolonged exposure to cadmium may cause renal dysfunction which may in turn lead to devastating bone disease in people with risk factors like poor nutrition. Populations that live in places polluted with cadmium often suffer from diseases like osteoporosis and increase risk of fractures. However, a link between exposure to cadmium and bone effects has also been noticed in people exposed to high concentrations of cadmium but not living in cadmium polluted areas (ATSDR, 2012).

Biomonitoring of Air Pollution

Monitoring of air pollution using bioindicators is evolving as a potentially effective and more economical alternative performing by direct ambient air measurements. This is especially relevant for monitoring large areas (Rühling, 1994). The usefulness of mosses in determining trace- and heavy-metal concentrations in different geographical areas has been discussed and demonstrated in several studies (Markert et al., 2003). Many European countries have used mosses since the beginning of 1960s in national and multinational surveys of atmospheric-metal deposition (Rühling, 1994). In practice, controlling anthropogenic air pollutants is a very complex problem where sources and emissions have to be managed and monitored, and economic aspects have to be integrated (Sloof, 1993). Biomonitoring is the one and only solution. In this study, the usefulness of biomonitoring as a technique used to investigate heavy metals atmospheric pollution is discussed.

Biomonitoring Concept

Biomonitoring is defined generally as the use of bio-organisms to obtain information on certain characteristics of the biosphere. The organism used is called a bioindicator or biological monitor (Markert et al., 1997). Bio-indicator generally refers to all organisms that provide information on the environment or the quality of environmental changes, and biomonitors are the organisms that provide quantitative information on the quality of the environment. Thus, with proper selection of organisms, air-pollution monitoring is possible even in remote areas as samples could be collected and measurements of pollutants done at laboratories miles away from the site. Even though there might be deposition of pollutants on the surface, these can be taken care of by proper washing of

13

samples before measurements (Markert et al., 2003). Biomonitoring is a passive method and provides a measure of integrated exposure over a period of time. The major advantages are:

1. No long term use of expensive sampling equipment is required.

2. Sampling of organisms used as biological monitor is generally easier.

3. The concentrations in the monitor organisms are higher than the system to be monitored. This improves the accuracy of measurements.

4. Most organisms reflect external conditions averaged over certain periods of time. This becomes important when monitoring levels change rapidly with time.

Biomonitoring of Air Pollution Using Moss and Lichen

Mosses and lichens are the plants which readily accumulate air pollutants (Bargagli, 1998). The results obtained from the differences between mosses and lichens as accumulator indicators depend on the species used in the studies, the type of emissions and environment in the studied area. The factors affecting the heavy-metal concentration in ground mosses and epiphytic lichens growing in the same place are canopy through-fall and stem flow (Poikolainen, 2004). The effect of through-fall on ground mosses varies and depends on whether the moss is growing under or between the crowns. In biomonitoring studies, moss samples are collected in open areas between the crown canopies in order to minimize the effect of through-fall. The amount of through-fall and stem flow varies according to the type of tree crown (Rasmussen, 1978). The crown canopy retains a part of the elements transported in free precipitation, but precipitation also leaches and washes off; e.g., nutrients from the canopy, which subsequently are absorbed by stem flow by epiphytic lichens.

14

No clear-cut evidence exists between lichen and moss, showing which could be a better heavy-metal biomonitor for regional surveys, because the results appear to vary from one place to another. However, the mechanisms through which mosses and lichens accumulate heavy metal are so different that they cannot be used to replace each another in national surveys. In Finland conditions, mosses appear to be more suitable for regional surveys than epiphytic lichens. (Wolterbeek et al., 1996) recommended the use of mosses because they more readily reflect local changes in heavy-metal deposition. However, lichens may be better accumulation indicators than mosses in arid conditions.

Biomonitoring Using Tree Rings

Tree rings widths are wider when conditions favor growth and narrower when conditions times are harsh. Other properties of the annual rings, such as maximum latewood density have been shown to be better proxies than simple ring width. Using tree rings, scientists have estimated many local climates for hundreds to thousands of years previously (Speer, 2010). By combining multiple tree-ring studies (sometimes with other climate proxy records), scientists have estimated past regional and global climates. Other advantages are:

1. Tree rings are especially useful as climate proxies in that they could be well-dated via dendrochronology (i.e. matching of the rings from sample to sample).

2. They are clearly demarked in annual increments, as opposed to other proxy methods such as boreholes.

In dendrochronology, the annual tree rings are used to determine the age of the tree by counting the number of rings. From the first ring, which is the pith and the center of the tree, to the last ring, the ring closest to the bark. The last

15

ring represents the present year if the sample is collected during or after the growing season of that year. However, if the sample is collected before the growing season the last ring would then be the year before the tree was fell (Speer, 2010).

Dendrochronology uses these annual tree rings as a natural proxy recorder for reconstructing historical environmental information. Proxy data are preserved physiological features in the environment, which could be used for meteorological measurements. Tree-ring parameters (ring width, density and isotopes) are being used as proxies for historical environmental information and could be used for reconstructing e.g. climate back in time. Ice cores, fossil pollen and oceanic sediments are other natural archives that are used for reconstructing historical climate (Fritts, 2012). There are two ways of collecting the tree-ring samples. Either by cutting the tree down or by using an increment borer to drill into the tree and withdraw a small transection of the tree.

In the latter method, it is important to have the borer in the same tilt as the stem. To be able to count all the tree-rings the borer must go through the middle of the tree, the pith (Speer, 2010).

One annual tree ring could be divided into two parts, earlywood and latewood. Earlywood, which is the lighter part of the wood, is produced in the spring and early summer when the growing season starts, and is less dense than the latewood which is produced late summer when the growing of the tree decelerates (Speer, 2010).

Tree rings are, in most cases, more distinct on trees growing in areas where there is a distinct seasonal difference in temperature and annual day length. In the tropical regions, the tree rings may be imposed by a wet and a dry

16

season instead of temperature difference. These tree rings are less noticeable compared to the trees growing in higher latitude such as boreal, temperate and sub temperate regions where annual climatological parameters create a bigger contrast between rings (Speer, 2010). Not only does the tree rings differ depending on what climate they are growing in, there is also a big difference in how well the tree rings are recognized between species. Swietenia macrophylla (Mahogany) which is a common species to use in dendrochronology, produces clear and well-marked tree-rings (Figure 12).

Other Studies Related to the Heavy Metal Pollution

The analysis performed on tree-ring metal concentration and isotope ratios of five stands located in three contrasted settings to infer the diffuse air pollution history of northern part of Canada. Tree-ring series shows that the Cd and Zn accumulation rate were higher between 1960 and 1968. The Pb concentrations indicate that the dominant source of lead from 1880 to the 1920s was the combustion of north-eastern America coal, which was succeeded by the combustion of leaded gasoline from the 1920s to the end of the 1980s (Annick et al., 2012).

Inductively coupled plasma mass spectrometry (ICP-MS) was used to examine trace element concentration in tree-rings over three and half centuries to assess macro-trends of environmental change. Tree-rings of a 350+ year old mammoth ponderosa pine (Pinus ponderosa) were analyzed for element concentration and evaluated versus local and global historical events. The ponderosa pine was located 100 miles south of the Canada/USA border and 180 miles east of the Pacific Ocean, and grew near apple orchards. The elements tested did not all display the same time versus concentration patterns. Copper

17

and chromium displayed cyclic concentration patterns over the last 350+ years, which appear to be associated with local events. Sr, Ba, Zn and Cd were found to be relatively constant between the mid-1600s and the early 1800s. Sr, Ba, Zn and Cd then increased beginning in the early 1800s for approximately 50 years then decreased to present day 2000 (Padilla & Anderson, 2002).

According to (Pumijumnong et al., 2001) trace elements (Cr, Co, Cu, Pb, Hg, Mo, Ni, Ti, W, U, and Zn) index in tree-ring wood was determined using high-resolution laser ablation inductively coupled plasma mass spectrometry (LA-ICP-MS). The accumulation of contaminants in tree-rings was affected by anthropogenic activities in the period 1958 to 2009, though signals varied in intensity with the distance of trees from the industrial plant. A stronger limitation of tree growth was observed in the proximity of the industrial plant in comparison with other pollutant sources. Levels of (Cr, Ni, Mo, V, U and W) increased in tree-ring profiles of trees close to the steel factory, especially during the 80's and 90's, in correspondence to a peak of pollution in this period, as recorded by air quality monitoring stations. The higher contents of Cu, Hg, Pb, and Ti could be related to the contaminants released from an incinerator located close to the industrial plant. The accumulation of contaminants in tree-rings reflected the historical variation of environmental pollution in the considered urban context

A study of elemental concentrations in tree-rings of pine along the past ten years from the template forests Desierto de los Leones, Villa del Carbon, and El Chico (reference or control site), in Central Mexico, was carried out to investigate the effect of atmospheric deposition on the trees. These sites were located within a 90 km radius from Mexico City. Elemental analyses were done with Particle Induced X-ray Emission (PIXE) spectrometry. The results showed

the major concentration in tree-rings corresponding to summer for elements S, Ni, Cu, and Zn (German et al., 2004).

Analytical Methods

Determination of the composition of ambient particulate matter involves the analysis of deposits collected. The chemical composition of particulate matter in ambient air provides essential information for assessment of contribution from different sources. For this reason, in this study analytical techniques used for the determination of elemental concentration in the tree samples is energy dispersive X-ray fluorescence (EDXRF) (Schwarze et al., 2006).

Other analytical techniques used for elemental analysis of particulate matter on filter materials are instrumental neutron activation analysis (INAA), inductively-coupled plasma with mass spectroscopy (ICP-MS), inductively-coupled plasma with atomic emission spectroscopy (ICP-AES), particle-induced X-ray emission (PIXE), proton (or particle) elastic scattering analysis (PESA), total reflection X-ray fluorescence (TRXRF), synchrotron induced X-ray fluorescence (S-XRF) and scanning electron microscopy with X-ray fluorescence (SEM/XRF). Brief descriptions of analytical techniques used in the studies on which this thesis was based would follow in subsequent subsections.

X-Ray Fluorescence Analysis

X-rays are electromagnetic radiation. All X-rays represent a very energetic portion of the electromagnetic spectrum and have short wavelengths of about 0.1 to 100 angstroms (Å). They are bounded by ultraviolet light at long wavelengths and gamma rays at short wavelengths (Brouwer, 2006). X-rays in

the range from 50 to 100 Å are termed soft X-rays because they have lower energies and are easily absorbed. X-rays have the following general properties:

1. Invisible and travel at the speed of light (3×10^8 m/s)

2. Not affected by both electrical and magnetic fields and capable of liberating photoelectron and recoils electrons

3. Differentially absorbed in passing through matter of varying composition, density and thickness

4. Reflected, diffracted, refracted and polarized and ionizing of gases is possible

5. Affect electrical properties of liquids and solids and blacken a photographic plate;

6. Emitted in both a continuous spectrum and with a line spectrum characteristic of the chemical element and have absorption spectra characteristic of the chemical element

X-ray Emission

X-rays are produced from the disturbance of the electron orbitals of atoms. This may be achieved in so many ways, the bombardment of a target element with high energy electrons is regarded as the most common. The first two are frequently used in X-ray spectrometry, either directly or indirectly. Electron bombardment results in both a continuum of X-ray energies and radiation that is characteristic of the target elements (Guthrie, 2012).
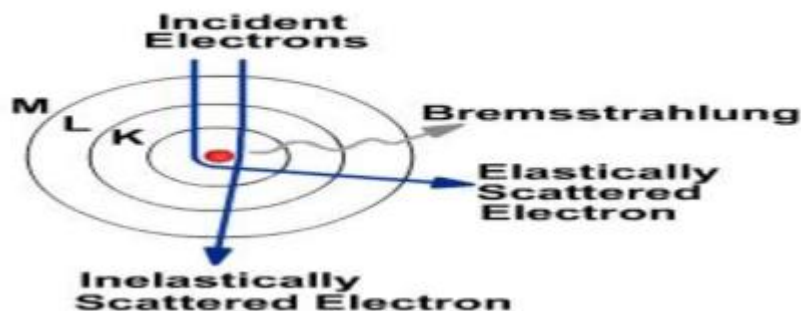
Figure 3: The Classical Model Showing the Production of Bremsstrahlung (NDT

resource center/march 2014. https://www.nde-ed.org)

Continuum X-rays

They are produced when electrons or high energy charged particles lose

energy in passing through the Coulomb field of a nucleus. In this interaction, the

radiant energy (photon) lost by the electron is called Bremsstrahlung as shown

in Figure 3. The emission of continuous X-rays finds a simple explanation in

terms of classic electromagnetic theory, since according to this; the acceleration

of charged particles should be accompanied by emission of radiation. In the case

of high energy electrons striking a target, they must be rapidly decelerated as

they penetrate the material of target, and such a high negative acceleration

should produce a pulse of radiation (Nave, 2013).

Characteristic Emission

The purpose of X-ray fluorescence is to determine chemical elements

both qualitatively and quantitatively by measuring their characteristic radiation.

To do this, the chemical elements in a sample must be caused to emit X-rays.

As characteristic X-rays only rise in the transition of atomic shell electron to

lower shell, vacant energy levels of the atom, a method must be applied that is

21

suitable for releasing electrons from the innermost shell of an atom. This involves adding to the inner electrons amounts of energy that are higher than the energy binding them to the atom. This could be done in a number of way which includes irradiation using elementary particles of sufficient energy (electrons, protons, a-particles) that transfer the energy necessary for release to the atomic shell electrons during collision processes, irradiation using X-ray or gamma-rays from radionuclides and irradiation using X-rays from an X-ray tube (Wittke, 2013)

Interactions of X-ray with Matter

When X-rays of intensity, I_0 are incident on an object of finite thickness, d, and density, ρ, the transmitted intensity of photons which have not suffered interactions, I, in the object is given by the Beer-Lambert law (Gerward, 1993) in equation 2.1.

$$I = I_0 e^{-\mu \rho d} \hspace{4cm} 2.1$$
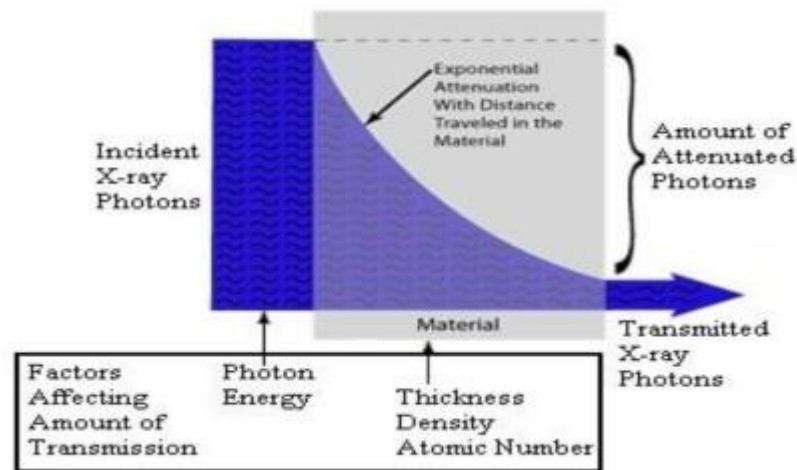
Figure 4: Exponential Attenuation of Photon Energy with Distance Traveled in the Material (NDT resource center/march 2014. https://www.nde-ed.org)

The linear absorption coefficient has the dimension [1/cm] and depends on the energy or the wavelength of the X-ray and the special density ρ (in gcm^{-3}) of the material that was passed through as shown in Figure 4. It is not the linear absorption coefficient that is specific to the absorptive properties of the element, but the coefficient applicable to the density ρ of the material that was passed through. The mass attenuation coefficient accounts for the various interactions and is therefore composed of here major components in equation 2.2

$$\mu(E) = \tau(E) + \sigma_{coh}(E) + \sigma_{inc}(E) \qquad\qquad 2.2$$

where $\tau(E)$ is the photoelectric mass absorption coefficient; $\sigma_{coh}(E)$ is the coherent mass absorption coefficient; $\sigma_{inc}(E)$ is the incoherent mass absorption coefficient.

Some of the photons interact with the particles of the matter and their energy could be absorbed or scattered. This absorption and scattering is called attenuation. Other photons travel completely through the object without interacting with any of the materials particles. The number of photons transmitted through a material depends on the thickness, density and atomic number of the material, and the energy of the individual photons. Even when they have the same energy, photons travel different distances within a material simply based on the probability of their encounter with one or more of the particles of the matter and the type of encounter that occur. Since the probability of an encounter increases with the distances traveled, the number of

photons reaching a specific point within the matter decreases exponentially with distance traveled (Gerward, 1993).

Energy Dispersive X-ray Fluorescence (EDXRF) Spectrometry

Energy-dispersive X-ray fluorescence (EDXRF) spectrometry exhibits several advantages over other methods that measure elemental content. This technique can measure numerous sample forms and can satisfy different measurement requirements (Wakisaka et al, 1996). Moreover, EDXRF spectrometry can detect a wide range of elements, even several elements simultaneously. This technique is nondestructive, fast, highly accurate, and environment friendly. EDXRF spectrometry can be used on different types of sample, such as bulk, liquid, powder, and gas. It can also detect particles in the air (Aboh, 2000; Cheung & Kong, 2002; Watson et al., 1999). EDXRF spectrometry can rapidly measure these harmful elements in products. This study introduces the theoretical analysis of energy dispersive X-ray, the internal structure of the EDXRF spectrometer, and the algorithm for the rapid analysis of multiple elements. This EDXRF equipment can measure minor elements in materials with contents below 0.03%.

Structure of the Energy Dispersive X-ray Fluorescence (EDXRF) Spectrometer

The EDXRF spectrometer is designed according to Moseley's law. The system is illustrated in Figure 5. The spectrometer consists of a power supply, a light path subsystem, a control circuit, and a personal computer (PC). High-voltage power is supplied to the X-ray tube to emit a primary X-ray, which irradiates the sample (Bandhu et al., 2000). The sample is then stimulated to

emit XRF, which is received by an XRF detector. The detector classifies the received photons according to energy and counts the number of photons that correspond to different energy levels. The detector then sends the results to the PC, which completes the qualitative and quantitative analyses.
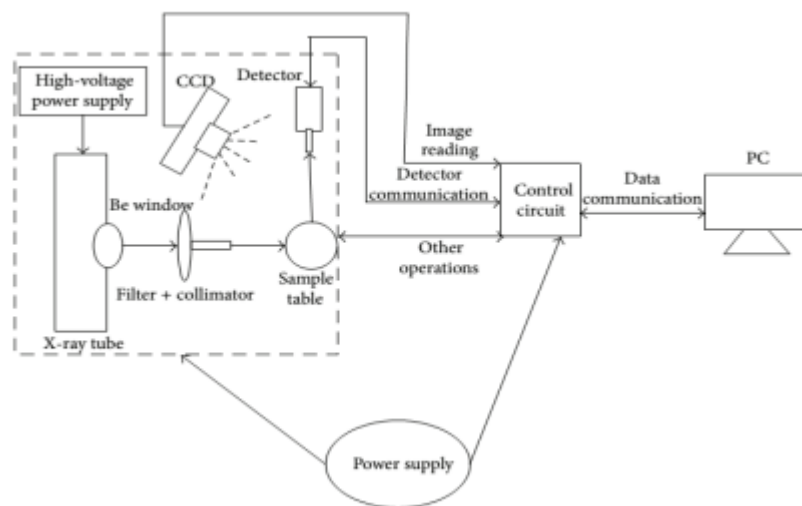
Figure 5: Structural Diagram of the Energy Dispersive X-ray Fluorescence spectrometer (Bandhu et al., 2000).

Light Path Subsystem

The light path subsystem, which includes the X-ray tube, filter, collimator, detector, and a charge-coupled device (CCD) camera, is shown in Figure 6. The light path subsystem is responsible for emitting, receiving, and counting the XRF photons. Its operation is as follows. A high-voltage power supply provides high voltage energy to the X-ray tube, which is stimulated to emit primary X-ray. The primary X-ray passes through the Be window, filter, and collimator, finally irradiating the sample. The sample is stimulated to emit XRF that can be recognized by the detector. The received XRF is transformed into a low-voltage pulse by the preamplifier. The pulse amplitude that is strictly proportional to the energy of the received. XRF is further amplified by the main

amplifier. The analog to-digital converter then transforms the amplified voltage into a digital signal. The digital signal is further shaped, sorted, and transformed into a pulse counter with amplitude information (Bandhu et al., 2000). This information is stored in a multichannel analyzer according to its amplitude and finally formatted to an XRF spectral line. The detector transmits spectral information to the PC through a USB hub in the control circuit for qualitative and quantitative analyses.
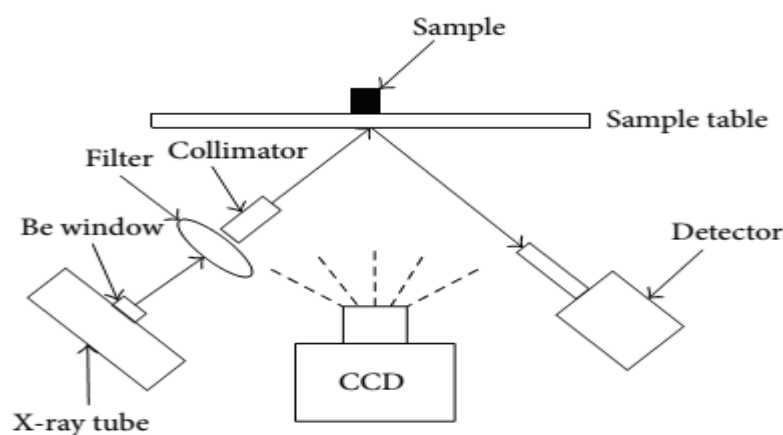
Figure 6: Structural Diagram of the Light Path Subsystem (Bandhu et al., 2000)

Figure 7: XY-501 X-ray Tube (Bandhu et al., 2000)

The X-ray tube in the light path subsystem (Model XY- 501; Dandong Oriental Electron Tube Factory, China) is shown in Figure 7. This X-ray tube can work at high voltage (50 kV) and low current (1 μA). It can also work at low voltage (4 kV) and high current (mA). This tube possesses good stability,

26

keeping low errors of 0.4% for 4 h. It has a small focal spot size, which is only 0.4 mm × 0.4 mm with a large X-ray flux. The detector (Model X-123; Amptek Company, USA) is the key part in the light path subsystem. This part mostly decides the performance of the EDXRF spectrometer.

The detector, which is actually a sensor, transforms photons to electrical pulse. The amplitude and number of electrical pluses are related to the energy and intensity of X-ray. The high-performance detector is shown in Figure 8.

The entire measurement is observed using a Charged Coupled Device (CCD) camera and sent to the PC. The control circuit is responsible for reading or setting the parameters of the tube pressure, switching the filter and the collimator, controlling the interlock, detecting motor position, receiving instructions from the PC, and controlling Universal Serial Bus (USB) communication.

Figure 8: X-123 Detector (Bandhu et al., 2000)

X-ray Fluorescence (XRF) Spectral Software

Qualitative analysis is performed to identify the elements in the sample. By contrast, quantitative analysis is used not only to identify the elements but also to determine elemental content. According to Moseley's law, the XRF photons of a certain element possess a fixed energy; that is, the XRF photons of elements are unique. The abscissa of a channel address reflects the photon

27

energy in the spectral line. The peak position of the abscissa corresponds to the energy of the characteristic XRF of a certain element. Channel address range of a detector in this system is designed from 0 to 2048. Each XRF photon energy ranges from 103 eV to 104 eV. Therefore, the enlargement factor of the energy/channel address is designed as 20 eV/channel. For example, the photon energy of $K\alpha$ for Ag is approximately 22.162 keV. The channel address should be near 1108 according to the energy calibration of 20 eV/channel. The K_α ray of Ag frequently appears in the channel address of 1106. (Gurol, 2008).

Qualitative Analysis

Qualitative analysis is the basis of quantitative analysis. Existing element types can determined using the former analysis. Qualitative analysis is generally divided into three steps.

1. Peak Location**.** The uncertainty of a large peak is approximately ±10 keV, whereas that of a small peak is up to ± 50 eV. Small peaks can be neglected when they overlap with a large peak, particularly when its energy level is below 12 keV. Spectral overlap and interference frequently occur in the K line (where the atomic number is between 22 and 35) and the L line (where the atomic number is between 56 and 96). All aforementioned factors hamper an accurate qualitative analysis.

2. Peak Recognition**.** The uncertainty of the peak position generally increases the difficulty of peak recognition. More than one peak corresponds to the energy peak in the spectrum in several cases. Accumulated, escape, and scattering peaks can also interfere with recognition.

3. Element Determination. Except for light elements, such as Na, Mg, Al, Si, P, and S, identifying an element typically requires more than two

28

characteristic spectral peaks. When the voltage of the X-ray tube is over 30 keV for atomic numbers Z = 19 to Z= 42, the spectral peaks K_α and K_β appear simultaneously. Furthermore, relative intensities in different spectral peaks should also be considered (Gurol, 2008). The characteristic peak area of the relative element in the qualitative analysis is calculated. This area corresponds to the photon number of the relative energy. The intensity of the characteristic peak can then be achieved. However, interference peaks should be considered in calculating the peak area. The peak in the peak location, which is an interference peak to the main peak, is called a pseudopeak. Such peak includes accumulated, escape, and scattering peaks. The accumulated peak is also called the sum peak, which is a phenomenon of peak hyperplasia resulting from the accumulation of signal pulses while counting at a high rate. In a sum peak, the peak position does not correspond to the characteristic energy but to the sum of two independent peak (Gurol, 2008).

When the energy of an X-ray photon is higher than the detection limit, some energy of the characteristic X-ray can escape because of its high transparency. The escaped energy forms an escape peak in the low-energy position. The energy difference between the main and escape peaks is equal to that of the energy of the characteristic X-ray photons, which is recognized by the detector. The Si-PIN detector shows that the escape peak energy is 1.74 keV lower than the main peak, which is the Si $K\alpha$ energy. The height of the escape peak is approximately 1/1000 to 2/100 of the main peak. However, the escape peak does not appear when the atomic number is over 30 (Sitko et al., 2009).

X-ray scatters when it passes through objects, and a scattering peak appears. Two types of scattering peaks are observed, namely, coherent

scattering (or Rayleigh scattering) and incoherent scattering (or Compton scattering). The scattering peak in the EDXRF spectrometer mainly results from the stimulation of the anode target of the X-ray tube.

Quantitative Analysis.

Quantitative analysis depends on the standard curve established by standard samples. The measured intensity value of the unknown element in an actual measurement is fed into the standard curve to obtain the elemental contents. In particular, the standard samples and unknown element should be measured under similar conditions (Bandhu et al., 2000).

Proton Induced X-ray Emission, PIXE

This is a technique whereby X-rays from inelastic collision of the projectile with inner core electrons are detected. PIXE is especially sensitive to trace elements and allows the determination of concentrations at a ppm level (Garman and Grime, 2005). However, PIXE generally does not yield depth information. When lower Z elements are detected, the preferred technique is PIGE. PIXE is one of the variants of X-ray emission techniques. This technique has also been used in the field of APM analysis (Lannefors et al., 1983) of PIXE, the ion knocks an inner-shell electron out of the atom and an X-ray is emitted as the vacancy is filled by an outer-shell electron. The energies of the X-rays are characteristic of the elements in the sample and the intensities of the X-ray lines could be used to calculate the concentration of the elements. This technique provides information on selected elements from Si to U with good sensitivity. Minimum detectable limits for PIXE analysis of aerosol samples are typically on the order of a few ngm^{-3} (Johansson et al., 1995).

A beam of energetic protons are accelerated onto a target (sample) of interest. This causes ionization and atomic excitation, leading to the ejection of inner-shell electrons from atoms in the target. The inner vacancies created are filled by outer shell electrons resulting in the emission of X-rays which are characteristic of the target's elemental composition and concentration. The X-ray spectrum is usually recorded in an energy dispersive mode using a Si(li) detector. The energies of the emitted X-rays are used to identify the atoms or elements in the target, and the X-ray intensities used to determine the element concentration. The PIXE facility, like any accelerator-based facility, consists essentially of ion sources, an accelerator system, a beam transport system, end stations (scattering chambers), and computer control system as depicted in Figure 9.
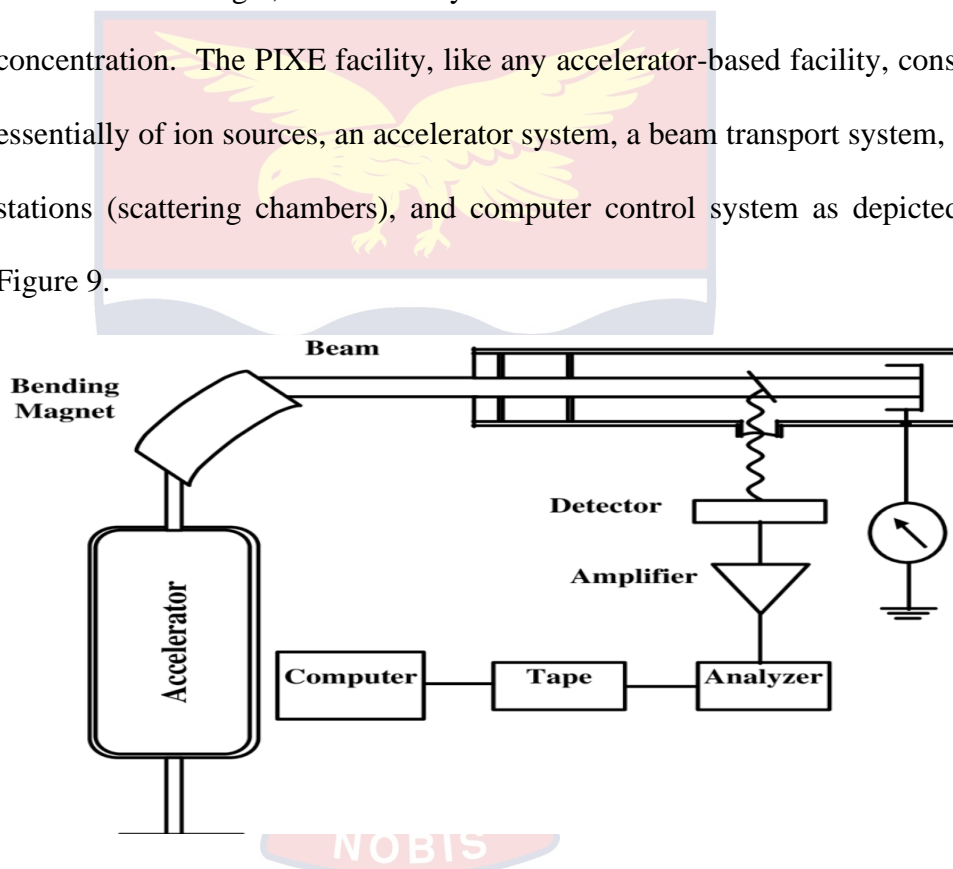
Figure 9: Schematic Diagram of Accelerator Set up

(http://www.wikimeda.com/August 2013)

Quantification Analysis Using PIXE

The main parameters needed to quantify the elements of interest in a sample is the number of X-rays from a transition j of the element z detected during PIXE measurement. It is known as yield and written as equation 2.3

$$Y_{OXj}(Z) = \sigma X_j(Z, E_O).\,\alpha Z.\frac{\Omega}{4\pi}.\,\epsilon_{det}\frac{Q}{e}.\frac{N_{Av}.\,(pt)Z}{A} \qquad 2.3$$

where: $\sigma X_j(Z, E_0)$ is the X-rays production cross section;

αZ is the fraction of transmitted X-rays from the target to the detector sensitive area;

Ω and ϵ_{det} are the solid angle covered by the detector and its intrinsic efficiency;

$(pt)_Z$ is the mean real density of the element Z in the surface impinged by the beam,

N_{Av} is the Avogadro number and A the atomic mass of the element Z.

Q is the integrated beam charge,

e the unit charge of the particles.

For a given X-ray, beam energy, detector, and measurement geometry, an efficiency factor η can be defined in equation 2.4:

$$\eta = \eta X_j(Z) = \sigma X_j(Z, E_O).\frac{\Omega}{4\pi}.\,\epsilon_{det}.\frac{N_{Av}}{A.\,e} \qquad 2.4$$

Equation 2.4 becomes

$$Y_{OXj} = \eta O.\,(pt)z \qquad 2.5$$

Provided η is known, the areal density $(pt)_Z$ of a given element can be obtained by measuring the corresponding X-ray yield on the detector and the integrated beam charge on the target. However, the efficiency factors $\eta(Z)$ are usually obtained experimentally using equation 2.5. This is performed by

irradiating elemental standards with known quantities $(\rho t)_Z$ of various elements and measuring the corresponding X-ray yields. The same conditions (same geometry and same beam energy) must be used for the standard and the samples to be analysed.

When a target cannot be assumed to be thin, corrections to the X-ray yield are required due to energy loss of the proton beam in the target matrix and attenuation of the emitted x-rays passing through the target. A matrix correction factor F_{xj} can hence be introduced. The factor is defined as the ratio between the ideal yield $Y_{OXj}(Z)$ that would be obtained from the same target, in the absence of matrix effects, and the actual yield, $Y_{Xj}(Z)$

$$F_{Xj}(Z) = \frac{Y_{OXj}(Z)}{Y_{Xj}(Z)} \qquad 2.6$$

Substituting equation 2.5 into equation 2.6 the corrected elemental area density $(\rho t)_z$ can be rewritten as equation 2.7

$$(pt)z = \frac{Y_{Xj}(Z)}{Q.\,\eta z.\,E_O} .\, F_{Xj}(Z) \qquad 2.7$$

According to Boni and Jex, apart from these low Z elements (Na, Mg, Al, and Si) which cannot be detected due to their self-absorption effects within the sample. The equation 2.7 could be used to approximate an aerosol sample to a thin target with the aim of simplifying the quantitative analysis, and apply the needed correction afterward (Boni et al., 1990; Jex et al., 1990).

Receptor Models

Receptor models are mathematical or statistical techniques used to identify and quantify the sources of airborne pollutants at a receptor or sampling site. The fundamental principle of receptor modelling is that mass conservation is assumed and on this basis a mass balance analysis could be used

33

to determine and apportion ambient PM concentrations to individual emitting sources (Hopke et al., 2006**).** Most receptor models used for source apportionment are in principle based on the assumption that the concentration of the pollutants measured at the receptor site is equal to the sum of the concentrations induced by the surrounding emission sources emitting the pollutants (Fabretti et al., 2009; Belis et al., 2013). The main objective of receptor models was, therefore, to identify the possible sources of particulate contaminant and to obtain data on their contributions to the bulk particle mass.

Enrichment factor analysis and multivariate techniques such as correlations and Positive Matrix Factorization (PMF) would be used to define a relationship between the sources and the receptor. These analytical methods would be used to combine and assist in the identification of sources and the apportionment of the observed pollutant concentrations to those sources in the urban area of Greater Accra, Ghana.

Positive Matrix Factorization (PMF)

PMF is used extensively for source apportionment of ambient particulate matter (Paatero & Tapper, 1994). PMF model resolves the dominant positive factors that contribute to PM samples without prior knowledge of the sources. This is achieved by using measured concentrations of PM to estimate the number of sources, the source composition, and the source contribution to each sample. The goal of PMF modelling is to

1. Determine the number of factors (sources or chemical/physical processes) that adequately explain the input data set variability and

2. Find correlation among the measured variables.

34

The advantages of the PMF relative to the traditional factor analysis methods such as Cluster Analysis (CA) and Principal Component Analysis (PCA) are unreliable data, such as observations below detection limit or missing values, could be included in the PMF analysis by giving them low weights to decrease their influence in the modelling (Paatero & Tapper, 1994). Data characterized by heavy positive skewed distribution could also be handled by down-weighting those extreme points to reduce undue influence in the model (Huang & Conte, 2009). PMF model assumes the non-negativity of factors and does not rely on information from the correlation matrix but utilizes a point-by-point least squares minimization scheme by taking into account the uncertainty of each data point (Pongkiatkul & Oanh, 2012).

Enrichment Factor (EF)

EF model helps to differentiate between elements originating from anthropogenic activities and those from natural sources. It is used mainly to provide an initial assessment on the degree of contributions from man-made activities to that of the measured atmospheric elemental concentrations. Consequently, it is used to estimate the degree of anthropogenic contamination. EF analyses have been extensively used in particle source apportionment studies to identify the major sources of air pollution and to quantify contributions of all sources of all measured pollutants (Chao & Wong, 2002; Cao et al., 2003; Zhang et al., 2008). The EF for each element at any sampling sites was calculated using the equation 2.8

$$\text{EF} = \frac{\left(\frac{\text{X}}{E}\right) tree\ ring}{\left(\frac{\text{X}}{\text{E}}\right) soil} \qquad 2.8$$

where X and E refer to the concentration (mg/kg) of the element of interest and the reference element respectively.

By definition, the enrichment factor closes to unity (EF = 1) indicates, that the element considered did originate from the soil (Chiarenzelli et al, 2001). The EF of an element is usually taken as being from a natural source if EF < 10. However, if EF > 10 then it is considered to indicate that a significant fraction of the element is contributed from anthropogenic source (Braga et al., 2005). EF values >100 and 1000 are taken as highly and heavily enriched respectively.

Chapter Summary

This chapter reviews literature related to the area of study. Two (2) sources of pollution (vehicular and industrial emission) were discussed. Rapid growths in population, urbanization, industrialization, and motorization have led to serious deterioration of the air quality in urban cities in developing countries like Ghana.

Increasing epidemiological evidence has established the adverse health effects associated with ambient air pollution. Monitoring of air pollution using bioindicators (mosses, lichens and tree rings) is evolving as a potentially effective and more economical alternative performing by direct ambient air measurements. The usefulness of tree rings in determining trace- and heavy-metal concentrations in different geographical areas has been discussed.

Determination of the composition of ambient particulate matter involves the analysis of deposits collected. The analytical techniques used for the determination of elemental concentration in the tree samples is energy dispersive X-ray fluorescence (EDXRF). This technique is nondestructive, fast, highly

accurate, and environment friendly as compared to other techniques. EDXRF spectrometry can be used on different types of sample, such as bulk, liquid, powder, and gas. It can also detect particles in the air. This EDXRF equipment can measure minor elements in materials with contents below 0.03%.

CHAPTER THREE

RESEARCH METHODS

Introduction

The research methodology primarily consisted of field work (sampling), laboratory experimentations and theoretical analytical methods. The samples were collected at Haatso-Atomic road and Tema industrial area in the Greater Accra region of Ghana. Swietenia mahagoni (mahogany), which is about one meter (1m) from the main road was logged and cross-sections taken. A total of 6 trees of Swietenia mahagoni were used. At both sampling sites, tree rings were counted, covering from 1957 to 2018 and 1968 to 2018. The results and observations recorded during the entire process are as presented and discussed in the sections that follow. In summary, the procedure and/or methodology employed to obtain the expected results of the research problem included:

i.   Sampling (i.e. sample collection using a increment borer and chain saw)

ii.   elemental analysis by EDXRF technique

iii.   Data analysis (i.e. statistical analyses were done by SPSS 16.0 software)

Study Area

Greater Accra region, the gateway to Ghana and home of our vibrant capital city, is one of the most exciting and distinctive regions. Although the smallest region, it is the most densely populated, containing the two great metropolitan areas of Accra and Tema, the country's major industrial and commercial centers.

38

Sites Location

Haatso is a town in the Ga East Municipal district. Haatso is located on this coordinate (5° 40′ 9.7″ N, 0° 12′ 27″ W) with a population of 18,000 people (CIA, 2016). The Haatso-Atomic road is adjacent to the Ghana Atomic Energy Commission (GAEC). Tema, on the other hand, is in Tema Metropolitan district and it is located 25 kilometers (16 miles) east of the capital city; Accra (5° 40′ 0″ N, 0° 0′ 0″ E) with a population of 292,773 people. Its modern industrial zone is one of our major commercial hubs. All samples analyzed for this study were taken from Haasto- Atomic road and Tema industrial area in the Greater Accra Region. The road side vegetation in the study sites are dominated by Azadirachta indica (Neem tree) and Swietenia mahagoni (Mahogany tree). These areas are well suited for the study of pollution effects because of the persistent vehicular traffic and industrial emission on the main roads. Figure 10a and Figure 10b respectively shows the map of Haatso-Atomic road and Tema industrial area, with sampling locations indicated in red circles along the main road.
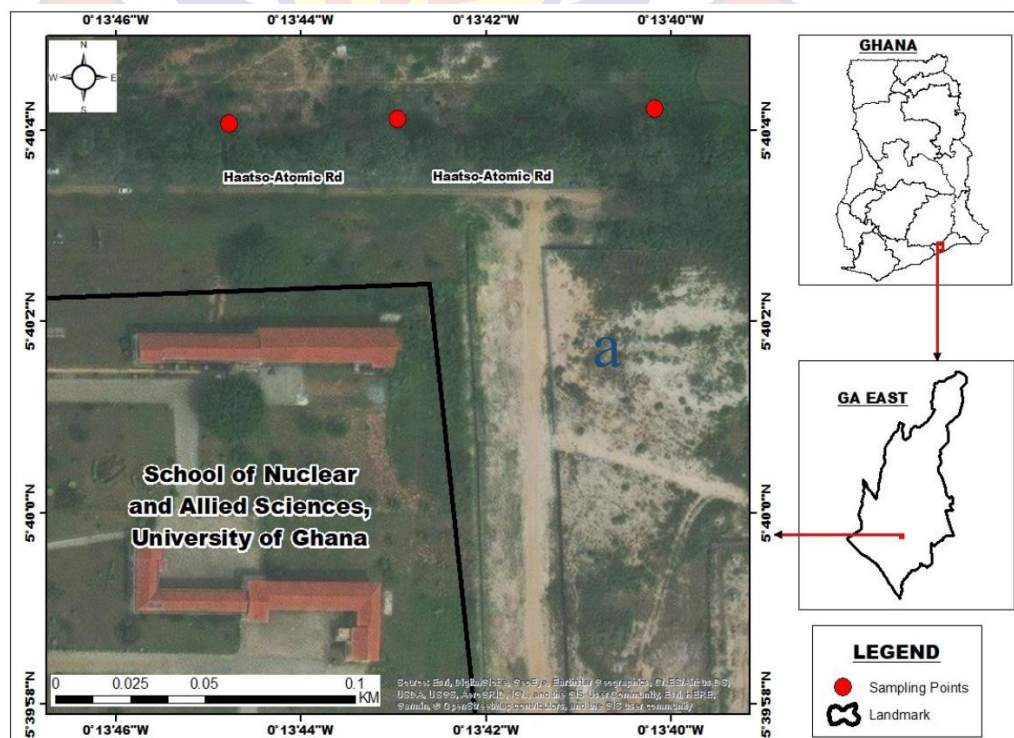
Figure 10a: Map Showing Sampling Site at Haatso-Atomic Road
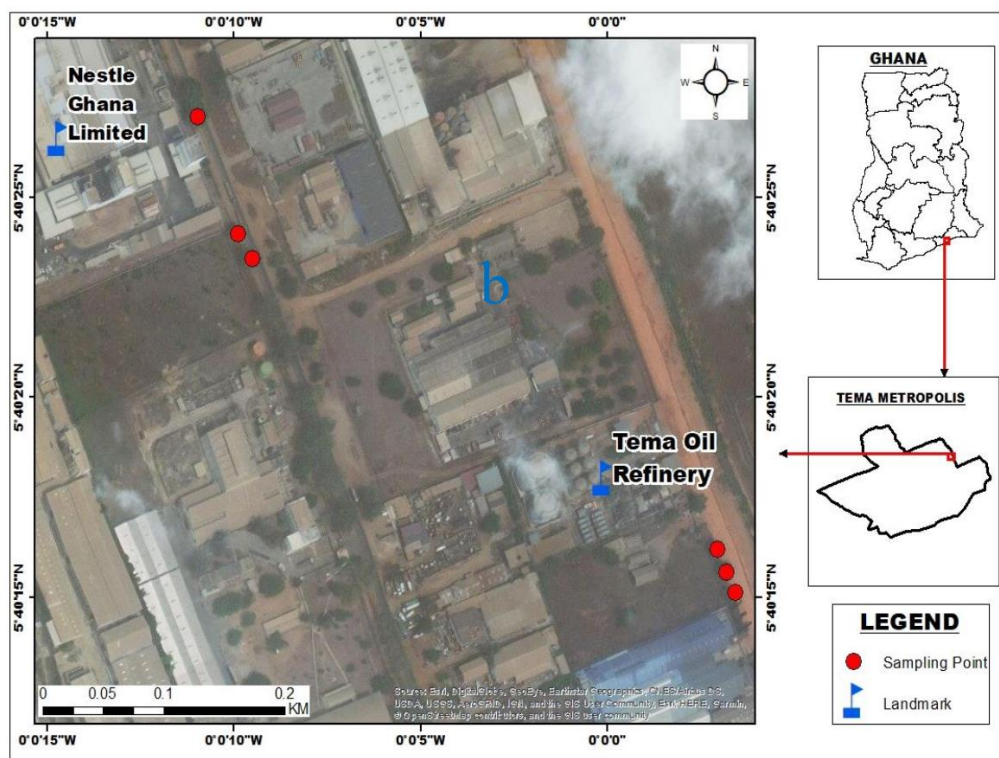
Figure 10b: Map Showing Sampling Site at Tema Industrial Area

Climate

Study areas were characterized by a tropical savanna climate under the Koppen climate classification. It lies in the driest part of Southern Ghana, experiencing average annual rainfall of about 750 millimeters (30 inch) (TMA, 2010). Average temperatures are high year-round, often exceeding 30°C. In Haatso, the mean monthly precipitation over the year, including rain and hail with average amount of annual precipitation is 31.89 inch (810.0 mm). The vegetation types are shrub lands and grassland.

Sampling Instrument and Samples

Increment Borer

The increment borer is essential for extracting a core of wood from trees, logs, poles or timbers. The core extracted is used for many purposes including determination of growth rate, age, trees soundness, penetration of chemicals in

the wood treating business, and specific gravity studies of wood. An increment borer consists of three parts. They are a handle, a borer bit and an extractor. When not in use, the borer bit and extractor fit inside the handle and form a compact unit. Most increment borers have Teflon coated bits. This coating helps reduce friction, protects against rust and keeps the bit cleaner and extends the life of the bit.
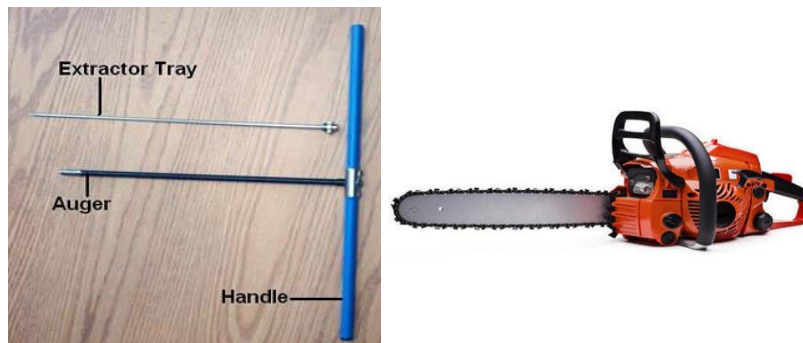
Figure 11: Increment Borer (left) and Chainsaw (right) used in the Study

Samples

The selection of samples in the present study was based on the role of the samples in the ecological system, availability of the samples in the vicinity of the roads and the ability of the samples being a bio-indicator. Swietenia mahagoni was chosen because it produces annual rings. In 2018, Swietenia mahagoni (mahogany), which is about one meter (1m) from the main road was logged and cross-sections taken for tree ring analysis as indicated in Figure 12a and Figure 12b respectively. The choice of this tree species was dependent on its ability to produce annual growth rings which is a prerequisite for trees being used as proxies.

41
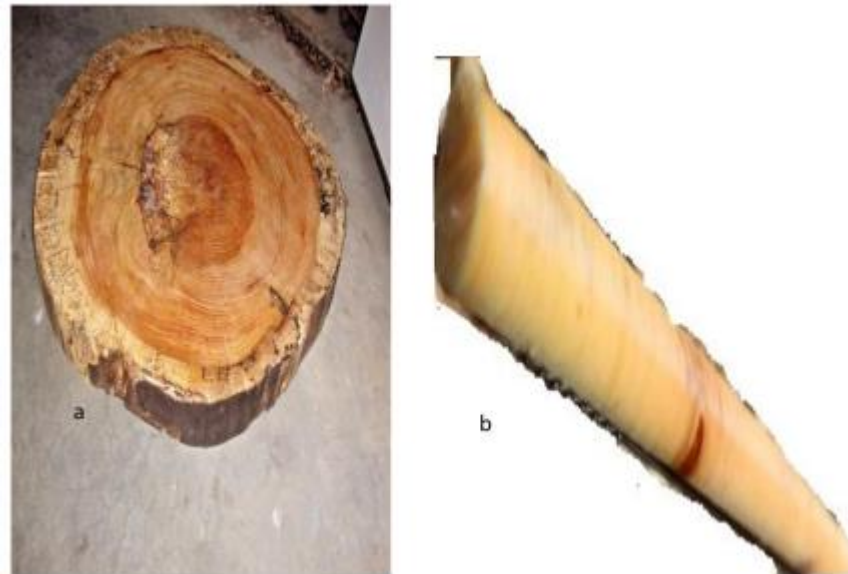
Figure 12: (a) Radial Cross-Section and (b) Radial Core of Swietenia Mahogani Tree

Preparation of Samples

a. Core sampling

1. A sharpened increment borer (10 mm in diameter) was used to extract cores from each stem.

2. The resulting core from the tree was removed using the extractor.

3. The extracted core was labelled with a specific ID and the procedure was repeated on the opposite side of the stem.

4. Then the samples were store in paper tubes to prevent any damage.

5. Finally, the cores were mount on wooden support beams and they were air dried for one week under control

b. Disc sampling

The sampled stumps or the fallen trees was divided into radial cross section using chain saw as indicated in Figure 13. The discs were label and stored in the laboratory. Radial subsections were sampled from these sections and the total length of each radial subsection from the pith to the cortex was 8mm.

Scanning

Wood samples were scanned at 1200–1800 dpi using a flatbed A3 scanner (Epson Expression 10000 XL).

Figure 13: Radial Cross-Section (Left) and Radial Core (Right) of Swietenia Mahogani Tree

Counting Analysis

After the cores and cross sections were scanned, visual dating and cross dating were done. The goal of cross dating is to assign calendar dates to each annual ring, and one way to start is to mark a visual ring count of the decades on the wood. A pencil was used to initially denote the decade's because you will probably need to erase and change them as you continue analysis. Since the tree was cut and bore in 2018, counting started from the pith, cores were marked from zero as the innermost ring of the tree with every tenth ring marked with a single pencil dot to designate the decade year. 61annual growth rings were

43

counted and the age of the tree could be estimated by subtracting 61 from 2018, which give us 1957 as the birth year of the tree at Haatso-Atomic road. The same tree ring counting analysis performed on Swietenia mahogani (Mahogany) from Tema industrial area, 50 annual growth rings were counted. Since the tree was bored with increment borer from the bark to the pith in 2018, the age of the tree could be estimated by subtracting 50 from 2018, which give us 1968 as the birth year of the tree analyzed.

Ring Width Measurement using Image J Software

A line was drawn from the left-hand edge of the image, parallel to the reference dots, to the right edge of the image (to the bark). The length of the line was set to 10mm. A series of dots displayed on image. Single dots were placed to represent each decade (Speer, 2011). The core of the sample was magnified using the glass icon and zoom icon. Since the rings are narrow, each tree-ring width in the sample was measured in succession from the inner most ring (left side of the image) toward the outermost one just inside the bark (right side of the image). The straight line measuring tool each time was re-position to measure with a line perpendicular to both sides of the ring. The results files were saved in an ".xls" format.

Energy-Dispersive X-ray Fluorescence (EDXRF) Principle

The samples were cut horizontally along their full length with a twin-blade saw to extract a 1.7mm thin wood brick with a width of approximately 10 mm. This was place in the energy dispersive sample holder. A current of 35A and voltage of 40 KeV were set first before the x-rays could be generated, the energy and intensity of x-rays that are generated depends on the amount of current and voltage that is applied to the x-ray tube. Our settings were adjusted

to measure the concentrations in milligram per kilogram (mg/kg). Which is how many times the XRF identifies a specific element on an area of 50μm during an 180seconds' exposure. Hay powder standard (IAEA-V-10) which contain known concentration of elements was analyzed. Figure 14 below shows the EDXRF machine that was used in carrying out this analyses.

Figure 14: EDXRF Machine used for Analyzing the Samples

As shown in Figure 15 the atoms in the sample were bombarded with primary X-rays, typically generated in an X-ray tube, hits an inner shell electron of the atom and ejects the electron from the atom. The open position is filled by an electron from a further outer shell and fluorescence radiation is emitted. The fluorescence energy is equal to the energy difference between the two electron shells. Therefore, the energy of this radiation is characteristic for the atom and indicates, what atom is present in the sample. As many atoms are present in the sample, it will emit various X-ray with different energy. The characteristic X-ray emitted was captured by the detector. The X-rays create signals in the detector, which are depending on the energy of the incoming radiation. The signals are collected in a multi-channel-analyzer.
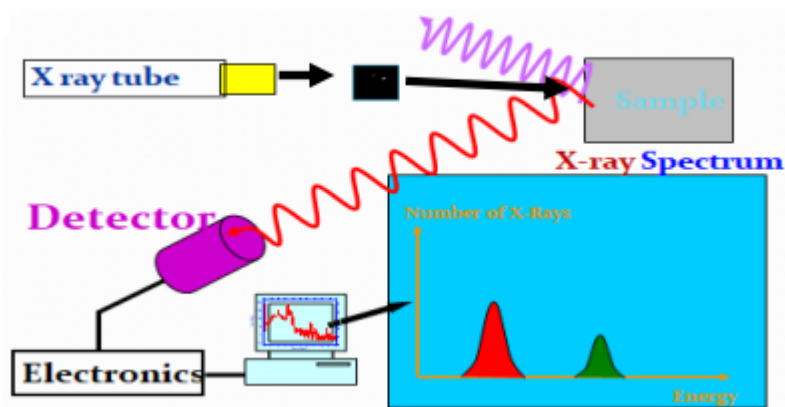
Figure 15: Schematic diagram of Energy Dispersive X-ray Fluoresence (https://www.researchgate.net/January 2013)

Qualitative Analysis

Qualitative analysis of X-ray spectroscopy is based on Moseley's law, and the energy equation is as follows:

$$E_X = RhC(Z - \sigma)^2 \left(\frac{1}{n_1^2} - \frac{1}{n_2^2} \right) \qquad 3.1$$

where E_X is the characteristic X-ray energy, R is Rydberg constant ($R\infty = 1.09737 \times 10^7$ m^{-1}), h is Planck's constant ($h = 6.6262 \times 10{-34}$ J·s), and C is the speed of photons. Z is the atomic number, σ is Shielding constant, and n_1 and n_2 are the energy series. For the spectrum $K\alpha_1$, shielding constant $\sigma = 1$, $n_1 = 1$ (K-shell), and $n_2 = 2$ (L-shell). Thus, equation (3.1) can be rewritten as follows:

$$E_{K\alpha1} = \frac{3RhC(Z - 1)^2}{4} \qquad 3.2$$

This law reveals the relationship between the X-ray energy and atomic number. This law is the theoretical basis for the qualitative analysis of material composition using XRF. A positive relationship exists between the count rate of the characteristic X-ray and the content of an element of the tested sample, is given in equation 3.3

46

$$I_K = \frac{KI_0}{\mu_0 + \mu_K} \times W_K \qquad\qquad 3.3$$

where I_K and I_0 are the K layer characteristics of the X-ray of the measured elements and the count rates of the incident X-ray, respectively. Moreover, μ_0 and μ_K are the absorption coefficients of the tested substance to the incident X-ray and the tested element to the layer K characteristic X-ray, respectively. K is the constant related to the specific measurement device and should be determined by the calibration instrument $KI_0 /(\mu_0 + \mu_K)$. WK is the measure of the content elements. Quantitative analysis of the measured elements using XRF is theoretically based on equation (3.3).

Element Determination.

Relative intensities in different spectral peaks was considered (Gurol, 2008). Figure 16 is the spectral line of Cu, Ni, Cu, Zn, Fe and Mn when the tube voltage is 40 keV and current is 35A. The characteristic peak area of the relative element in the qualitative analysis is calculated. This area corresponds to the photon number of the relative energy. The intensity of the characteristic peak can then be achieved. Raw data was then summarized in an Excel sheet displaying rarities location of element in the sample. The results are presented in appendices 1 to 2.
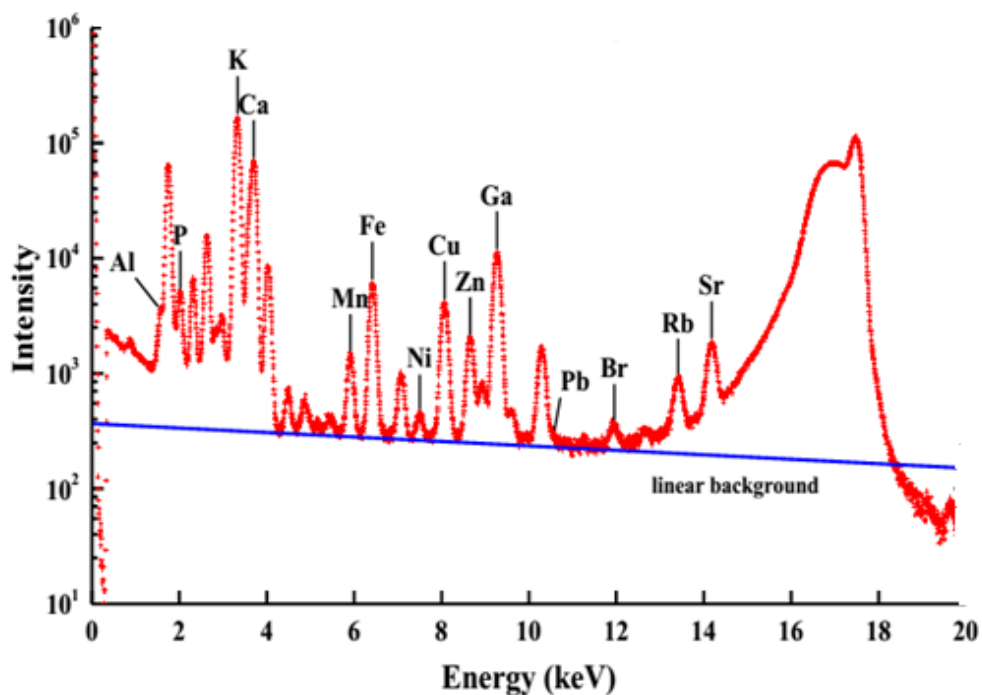
Figure 16: Spectral Line of Elements

Quantitative Analysis

Quantitative analysis depends on the standard curve established by standard samples. The measured intensity value of the unknown element in an actual measurement is fed into the standard curve to obtain the elemental contents which are illustrated in Figure 17. In particular, the standard samples and unknown element should measure under similar conditions. Detailed steps are illustrated in Figure 17
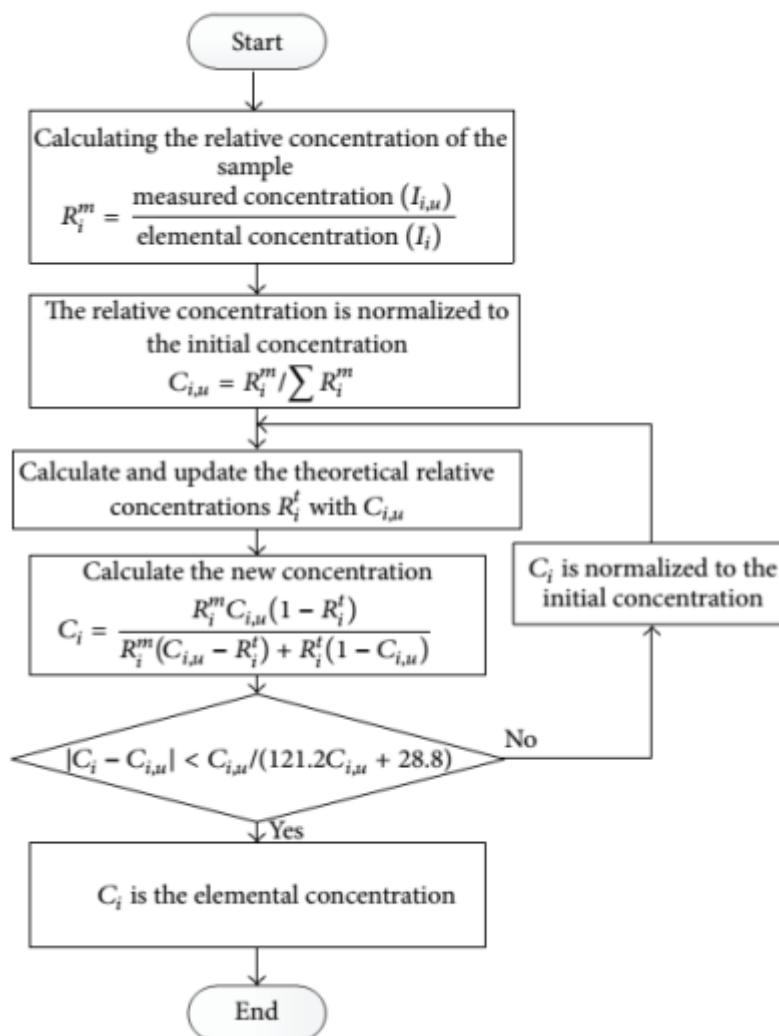
Figure 17: Steps of Quantitative Analysis

Measurement started after the suitable working mode has been established. Figure 18 presents some results of the quantitative analysis, which show some elements of Cu, Zn, and Pb with their content of 9.62 mg/kg, 15.78 mg/kg and 0.11 mg/kg respectively. Raw data was then summarized in an excel sheet and the concentration was measured in milligram per kilogram (mg/kg). Experimental results are presented in appendices 1and 2.
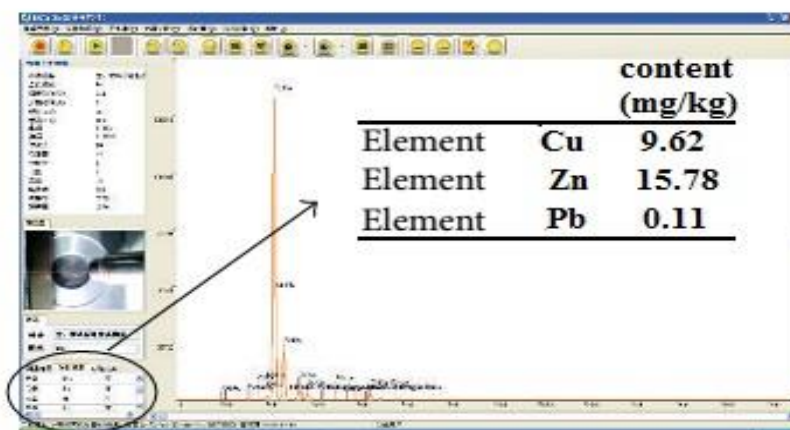
Figure 18: Results of the Qualitative Analysis

Data Analysis

Pearson's correlation coefficient (r) is a measure of the strength of the association between the two variables. Statistical analysis of the data was carried out using Pearson's correlation coefficient to determine the association between the heavy metals and ring width at the two sampling sites to achieve the specific objectives of the study. All statistical analyses were done by Statistical Package for Social Sciences (SPSS 16.0) software.

Chapter Summary

This chapter discusses the methods and materials used to obtain the results. Pearson's correlation coefficient was used to determine the association between the heavy metals and ring width at the two sampling sites. The samples were collected at Haatso-Atomic road and Tema industrial area in the Greater Accra region of Ghana. Swietenia mahagoni (mahogany), which is about one meter (1m) from the main road was logged and cross-sections taken. A total of 6 trees of Swietenia mahagoni were used. At both sampling sites, tree rings were counted, spanning from 1957 to 2018 and 1968 to 2018. EDXRF spectrometer was used to investigate the presence of heavy metals in tree rings.

50

CHAPTER FOUR

RESULTS AND DISCUSSION

Introduction

The heavy metal markers chosen to monitor atmospheric pollution from vehicular and industrial sources were Zn, Cu, Cd, Mn, Ni, Fe and Pb. Growth rates measured from tree rings were compared with precipitation data from the Meteorological stations in Accra and Tema.

Growth Rates of Trees at Haatso-Atomic Road
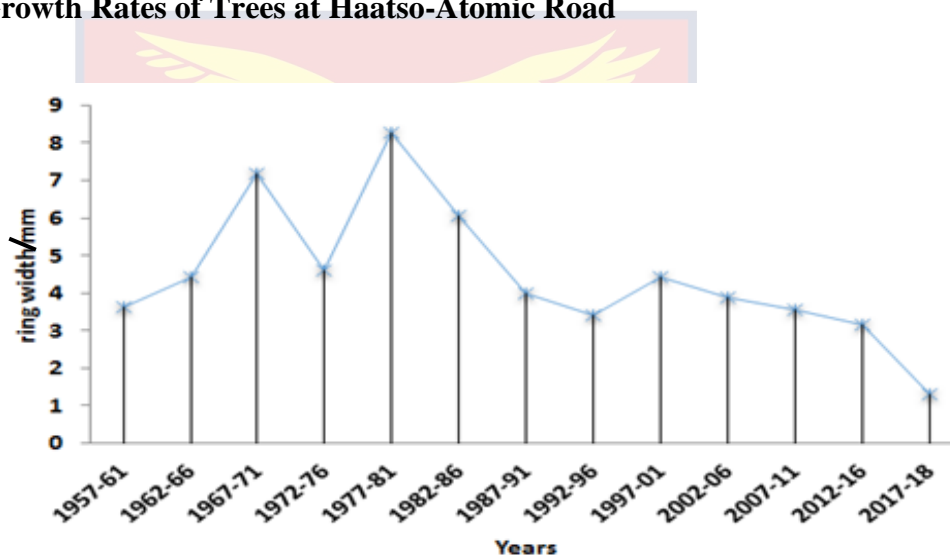
Figure 19: Plot Showing Tree Ring Widths Averaged Over Five-Year Period.

From Figure 19, it was observed that there was a consistent increase in growth of the tree from 1957 to 1971, after which there was a sudden sharp decline of growth, which could be attributed to harsh environmental conditions such as drought which inhibits growth. From 1977 to 1980, there was an average growth of the tree which was the highest life time growth recorded for the tree thus 8 mm growth. Soon after this growth there was long period of decline till 2018 when the tree was logged. This prolong period of decline in growth could only be attributed to harsh seasonal variations or heavy metal pollution from vehicular emission.

51

Figure 20, further illustrate the growth rate patterns for the tree analyzed over the period of 1957 to 2018. Negative growth was observed in 1974, 1984 and 2018. The negative growth in 2018 raised lots of concerns since vehicular emission have increased steadily over the last decades.
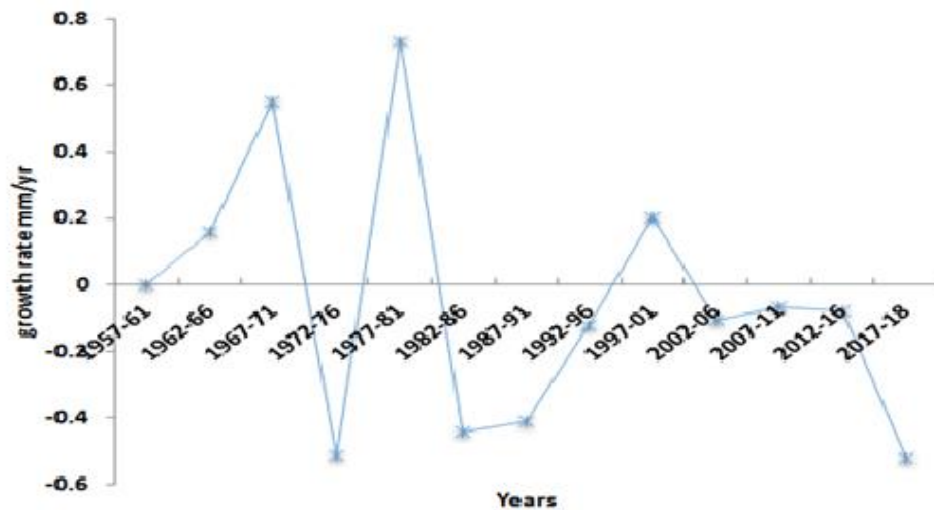
Figure 20: A Plot Showing Growth Rates of Trees Over 61years Period (1957-2018)

Tree Ring Growth and Climate Relationship

From Figure 21, which shows the annual ring width for the tree sample, some years recorded very high growth whiles others experienced a sudden steep dip in growth. Tree growth rings were compared with annual wet and dry events recorded by the meteorological Agency for Accra. Figure 21 is compare with precipitating levels (Table 1) with levels (above 60 mm and below classified as wet and dry respectively). The years 1965, 1968, 1970, 1975, 1979, 1983, 2011 recorded very high growth, which could be attributed to conducive environmental conditions such as enough rainfall during those years.

52
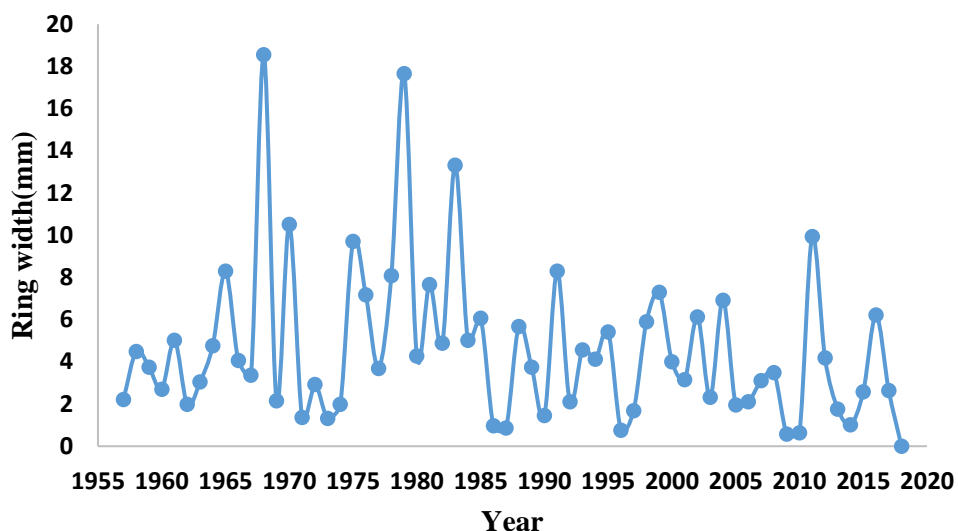
Figure 21: Illustration of Annual Ring Width Estimated for the Tree.

Table 1: Classification into Wet and Dry Rainfall Years from Meteorological stations in Accra

Year	Accra rainfall(mm)	Year	Accra rainfall(mm)
1965	87.84(wet year)	1976	45.80(dry year)
1968	117.73(wet year)	1977	31.09(dry year)
1970	74.51(wet year)	1978	44.78(dry year)
1975	74.31(wet year)	1983	58.76(dry year)
1979	76.45(wet year)	1992	46.42(dry year)
1983	77.76(wet year)	1993	40.73(dry year)
2011	84.53(wet year)	1994	45.66(dry year)
2016	81.69(wet year)	1998	42.80(dry year)
		2000	42.68(dry year)

Elemental Composition of Tree Rings at Haatso-Atomic Road

Copper Concentration

Copper concentrations were determined for annual rings sampled from the logged tree which spanned from the years 1957 to 2018. The average copper concentration in the annual rings measured (1957 to 2018) ranged from 3.15 – 9.86 mg/kg. These values were below the limits set by WHO for copper levels in plants which is 10mg/kg (Zigham et al., 2012)**.** From Figure 22 the concentration of copper started rising from1957 to 1984, and fluctuated from 1984 to 1988 and followed an increased in trend till 2017. The amount of copper, however, reached a peak in 2017 of a value of 9.86 mg/kg. The consistent increase in the levels of Cu could be attributed to the increase in vehicular traffic activities on the stretch of road where the samples were taken; Cu pollution from vehicles has been linked to wear of brake lining (Vecchi et al., 2007). Copper and zinc have been definite to be a good indicator of traffic emissions from brake wear and tear matter emissions.
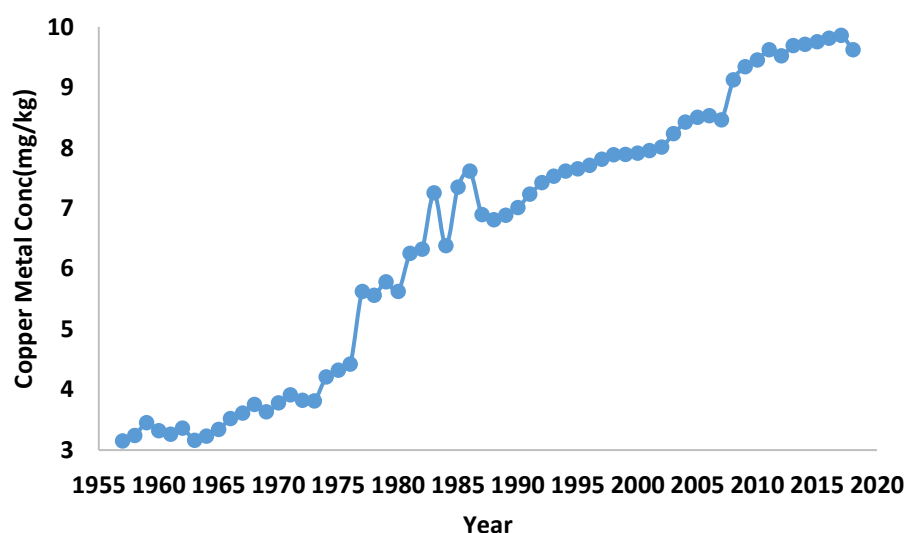
Figure 22: Copper Concentration at Haatso-Atomic Road

54

Zinc Concentration

Zinc concentrations ranged between 8.18 – 15.78 mg/kg as shown in Figure 23. The concentrations of zinc fluctuated from the year 1964 to 1999. The highest concentration of Zinc was recorded in 2018 with a concentration of 15.78 mg/kg. The zinc values recorded at the site were below the WHO's recommended maximum limit of zinc in plants which is 50 mg/kg (Afzal-Shah et al., 2011). The consistent increase in the levels of Zn could be attributed to wears of brakes and tires from vehicles plying that road.
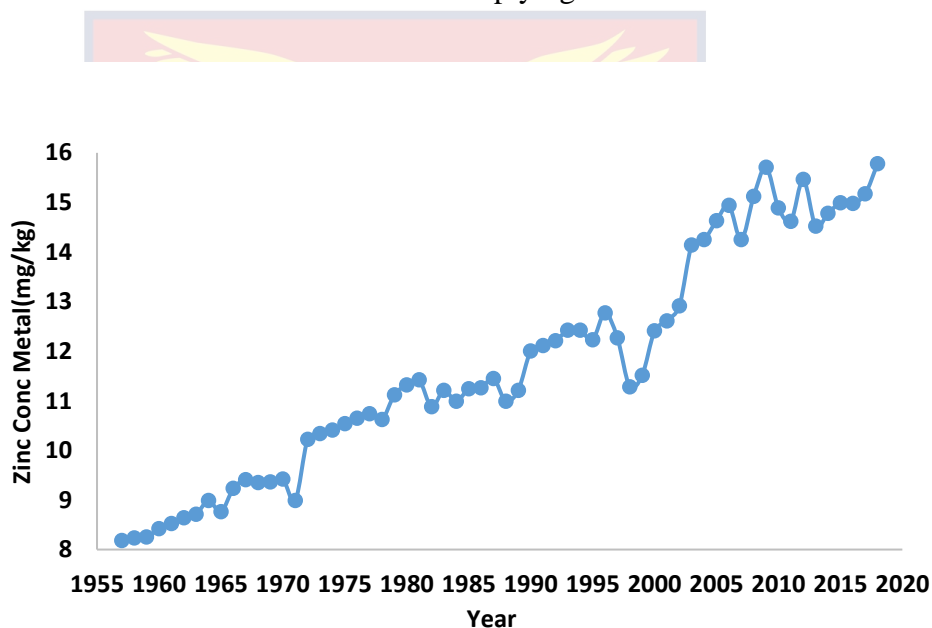
Figure 23: Zinc Concentration at Haatso-Atomic Road

Lead Concentration

From Figure 24, there was a characteristic rise and fall in lead from 1957 to 1982 in which lead increased sharply and decreased in trend till 2018. The highest amount of lead was 0.60 mg/kg recorded in 1986. The maximum limit of lead in plants, recommended by WHO, is 2 mg/kg (Afzal-Shah et al., 2011). Before the phasing out of leaded fuels, lead concentrations in the ambient air ranged from 2 µg/m³ to 188 µg/m³ (2000- 188000 ng/m³) which was above annual EPA

55

Ghana guideline value of 2.5 µg/m³ (2500 ng/m³). After the phase out of lead in gasoline, lead concentrations ranged from 0 – 1.97 µg/m3 (0 – 1970 ng/m³) (Nerquaye-Tetteh, 2009). A study conducted by (Safo-Adu et al., 2014) also revealed low particulate lead levels in the ambient air along the Accra-Tema Highway. The low lead levels recorded in this study thus confirmed a positive phase out of the use of leaded fuel. Its (lead) widespread in the environment is as a result of its former use as an additive in fuel as well as its use in paints (ATSDR, 2007). Pb remains a major public health issue in countries of most developing world due to the differences in the sources as well as pathways of exposure. At high exposure levels, most organs and systems such as the kidneys and central nervous systems are injured. However, at lower levels, 'haeme synthesis and other biochemical processes are affected, psychological and neurobehavioural functions are also impaired' (Tong et al., 2000).
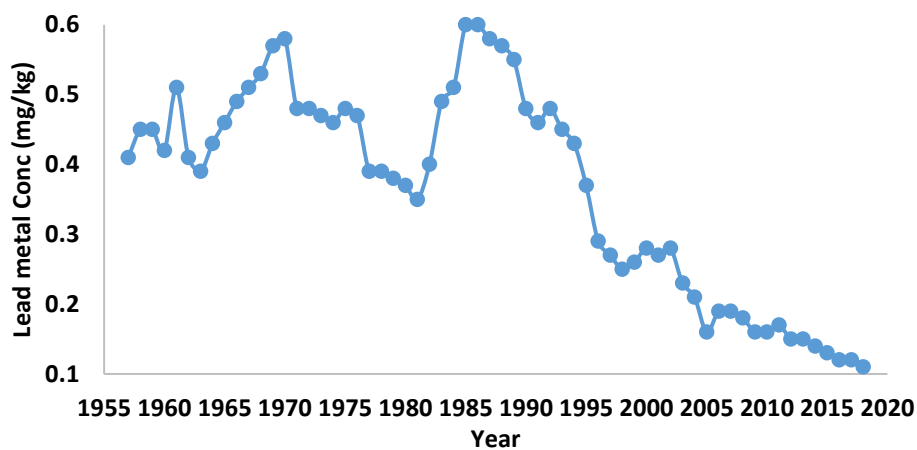
Figure 24: Lead Concentration at Haatso-Atomic Road

Cadmium Concentration

From Figure 25, there was a characteristic rise and fall in cadmium from 1957 to 1995 in which Cd sharply increased and decreased. The highest concentration of cadmium (0.09 mg/kg) was recorded in 2018. The maximum limit of Cd in plants, recommended by WHO, is 0.02 mg/kg (Afzal-Shah et al., 2011). The presence of cadmium at the sampling site may be accredited to vehicular exhaust emission due to its existence in gasoline and as an effect of corrosion of car parts as established by the European Commission, 2001. Potential sources of cadmium include vehicular exhaust emissions of tire abrasion; open burning of municipal wastes containing Ni-Cd batteries from vehicles (Awan et al., 2011).
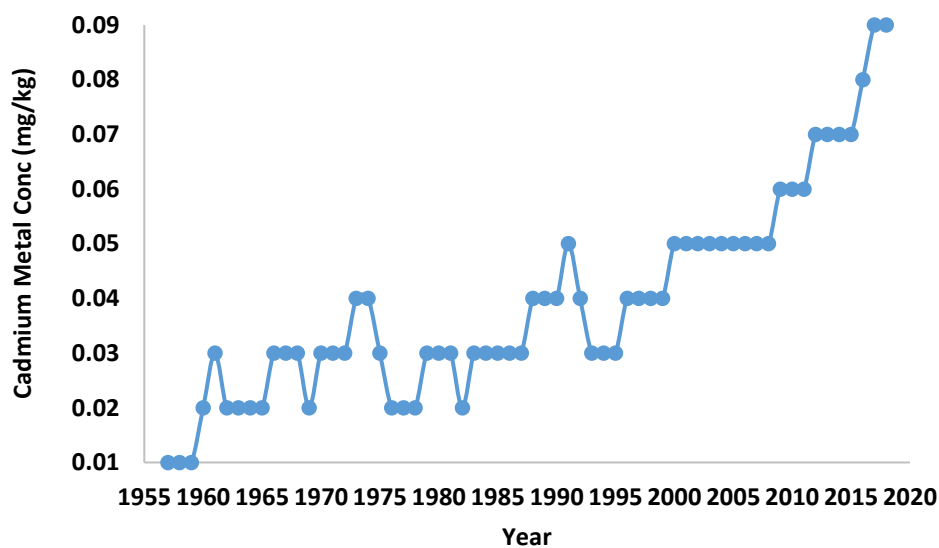
Figure 25: Cadmium Concentration at Haatso-Atomic Road

Manganese Concentration

Manganese concentrations ranged from 2.58 – 5.94 mg/kg as shown in Figure 26. There was a fluctuation in manganese from 1957 to 2011 after which there was an increased in trend till 2018. The highest concentration of manganese (5.94 mg/kg) was recorded in the year 2018. The manganese values

57

recorded at the site was above the WHO guideline values of 2.14 mg/kg (Afzal-Shah et al., 2011). Manganese concentrations were predicted to be high due to the Methylcyclopentadienyl Manganese Tricarbonyl (MMT) additive in fuels.
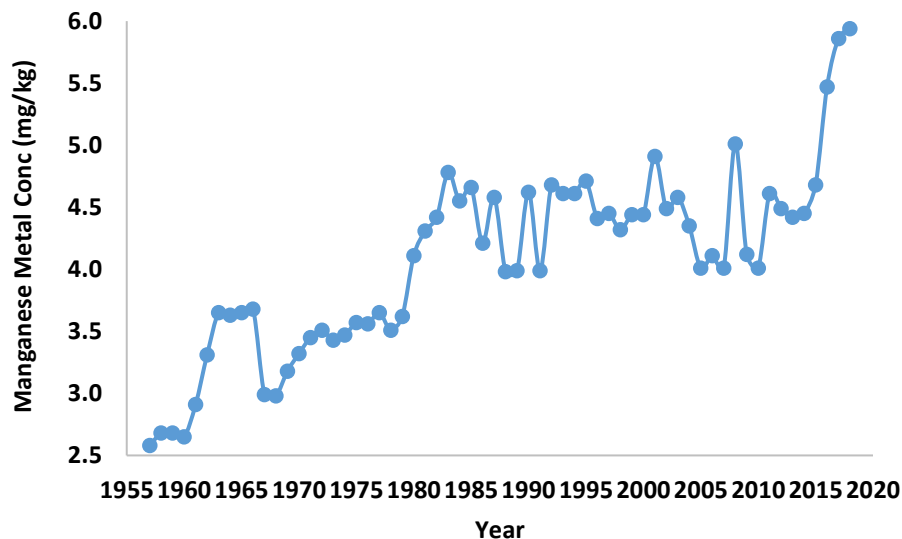
Figure 26: Manganese Concentration at Haatso-Atomic Road

Nickel Concentration

Concentration of Ni ranged from 0.10 – 0.99 mg/kg as shown in Figure 27. The concentration of nickel increased from 1957 to 2018. The highest amount of 0.99 mg/kg was recorded in 2018. The nickel concentrations recorded for Haatso-Atomic road were above the WHO's recommended limit of nickel in plants of 10 mg/kg (Zigham et al., 2012**).** Nickel mostly has been associated with combustion of diesel which has been on the rise as the number of vehicles on our road **(**Ya-Fen Wang, 2003).
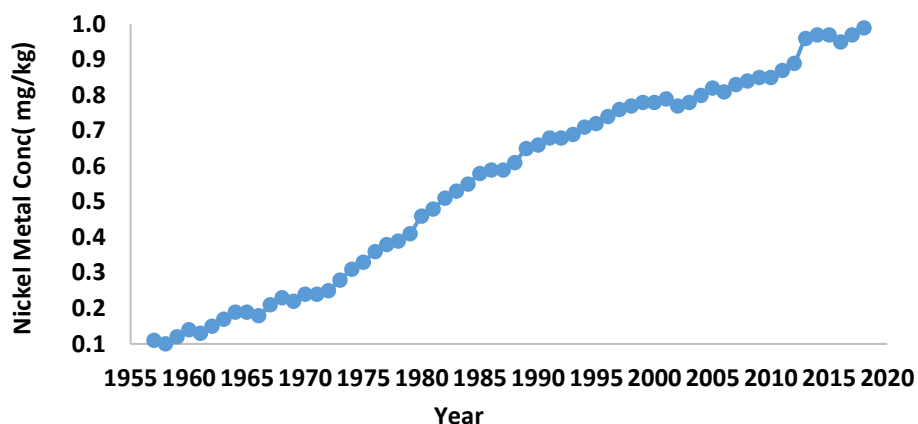
Figure 27: Nickel Concentration at Haatso-Atomic Road.

Comparison of Growth Width of Trees from Haatso and Tema Industrial Area

The growth trend of tree ring widths from both sampling locations was compared. Since the same species of tree was used for monitoring at both site locations, and both locations are in Accra and shared fairly similar weather conditions, differences in the growth patterns could be attributed to external environmental factors such as pollution. From Figure 28, growth trends were similar from 1969 to 1999; and it was observed that there were increase and decline of ring width during these periods. From 1999 to 2018, there was a constant decline in growth from the tree from Haatso whiles there was an increase in growth at the industrial area. This trend could be attributed to the increase in the number of vehicles utilizing the Haatso Atomic road; the past decade has seen an astronomical increase in traffic density on that stretch of road. From literature, some researchers have attributed the decline in growth of trees to the increasing levels of pollution from vehicular emissions. The increase in the growth of trees along the industrial area of the country could be attributed to low production from these industries as results of frequent power outages over the past decades. One could also observe lower levels of pollutants in the trees

59

from the industrial area which could be attributed to the stern regulations and monitoring implemented by the environmental protection agency on industrial emissions.
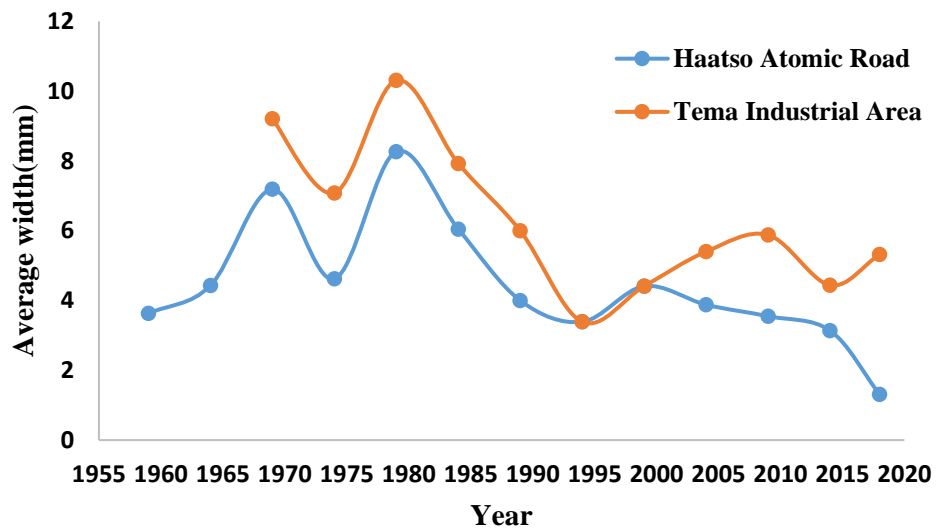
Figure 28: Comparison of Growth Between Mahoganies at Haatso Atomic Road and Tema Industrial Area

Elemental Composition of Tree Rings at Tema Industrial Area

Zinc Concentration

Zinc concentrations were determined for annual rings sampled from the logged tree which spanned from the years 1968 to 2018. Zinc concentrations ranged between 5.37 – 13.9 mg/kg as shown in Figure 29. The concentration of zinc increased from 1968 to 1976 followed a decrease to 1982. Suddenly, Zn became constant from 1985 to 1992 and increased in concentration from 1993 to 2005. The highest concentration of Zinc was recorded in 2005 with a concentration of 13.9 mg/kg. The zinc values recorded at the site were below the WHO's recommended maximum limit of zinc in plants which was 50 mg/kg

(Afzal-Shah et al., 2011). In this study, observed concentrations of zinc at the industrial area could be attributed to coal combustion and steel industry.
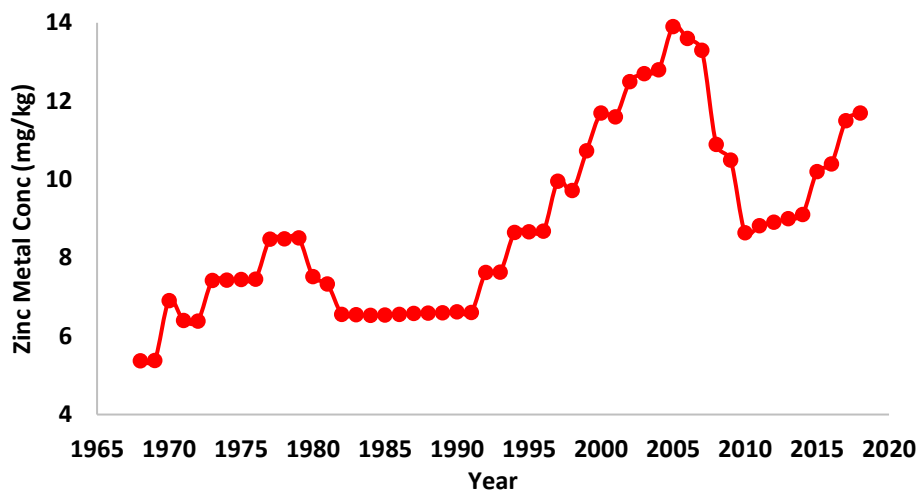
Figure 29: Zinc Concentration at Tema Industrial Area.

Lead Concentration

From Figure 30, lead started increasing from 1968 to 1970 and there was a decline from 1971 to 1980. Lead fluctuated from 1981 to 2018. The highest amount of Pb was 0.45 mg/kg recorded in 1970. The maximum limit of lead in plants, recommended by WHO, are 2 mg/kg (Afzal-Shah et al., 2011). Pb values were high in 1970, 1986 and 1992, the industries located at the sampling site do not emit lead. But consistent decrease in the levels of lead confirms a positive phase out of the use of leaded fuel in vehicles
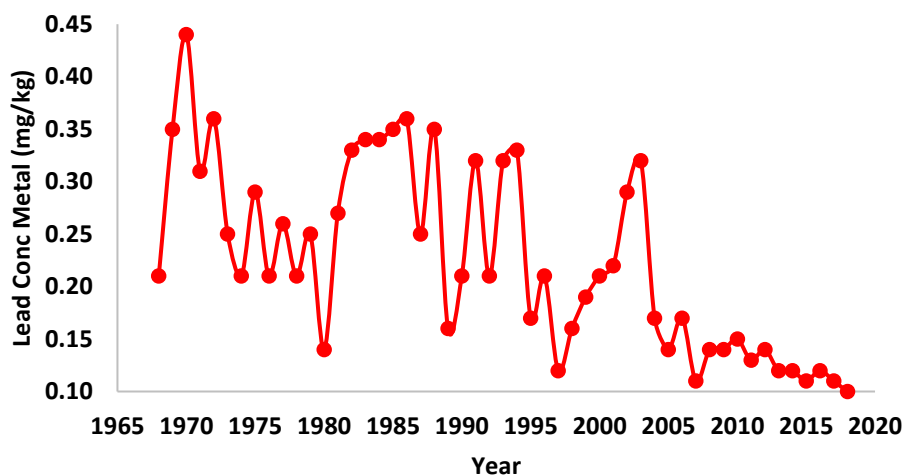
Figure 30: Lead Concentration at Tema Industrial Area.

Copper Concentration

The average copper concentration in the annual rings measured ranged from 1.92 – 6.70 mg/kg. Although these values were below the limits set by WHO for copper levels in plants was 10 mg/kg (Zigham et al., 2012). This study attempts to identify the trend in these Cu levels over the past 50 years in order to answer some relevant questions whether recent activities in the millennium has really contributed to the current global pollution levels. From Figure 31, the concentration of copper started rising at 1968 to 2014, then followed an increase in trend till 2018. The amount of copper, however, reached a peak in 2017 of a value 6.70 mg/kg. The consistent increase in the levels of Cu can be attributed to the electrical copper wire production industry on the stretch of road where the samples were taken; Cu pollution from vehicles has been linked to wear of brake lining (Vecchi et al., 2007).
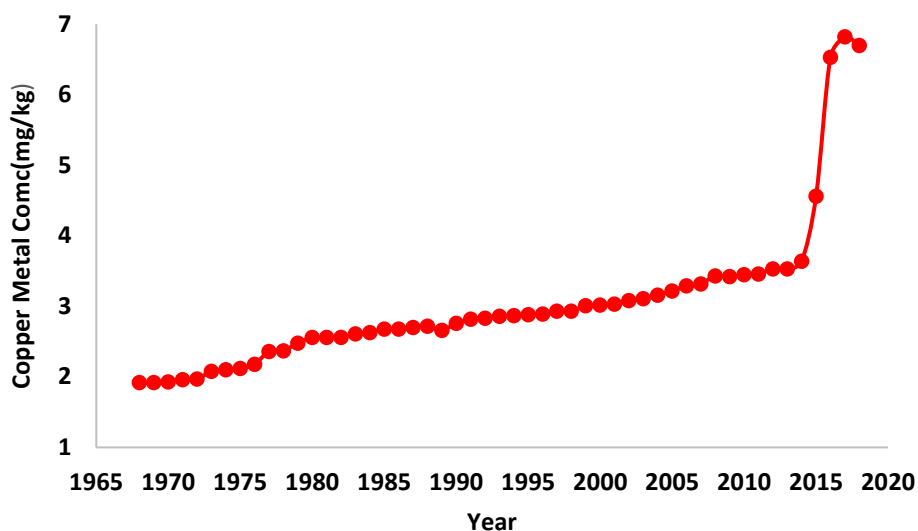
Figure 31: Copper Concentration at Tema Industrial Area.

Iron Concentration

As the data show, in Figure 32, the amount of iron concentration fluctuated from 1968 to 1988 then followed a decrease in trend till 1993. There was a sharp increase from 1994 to 1996, followed by variation from 1997 to 2018. The highest concentration value was 90.1 mg/kg which corresponded to 1996. The WHO recommended level of iron in plants was 20 mg/kg (Afzal-Shah et al., 2011). Iron values recorded at the industrial area were above WHO recommended levels and this could be credited to road dust and iron and steel industry. In vehicles, iron (Fe) pollution was from the wear and tear of brake pads and other automobile parts (Schauer, 2006).

63
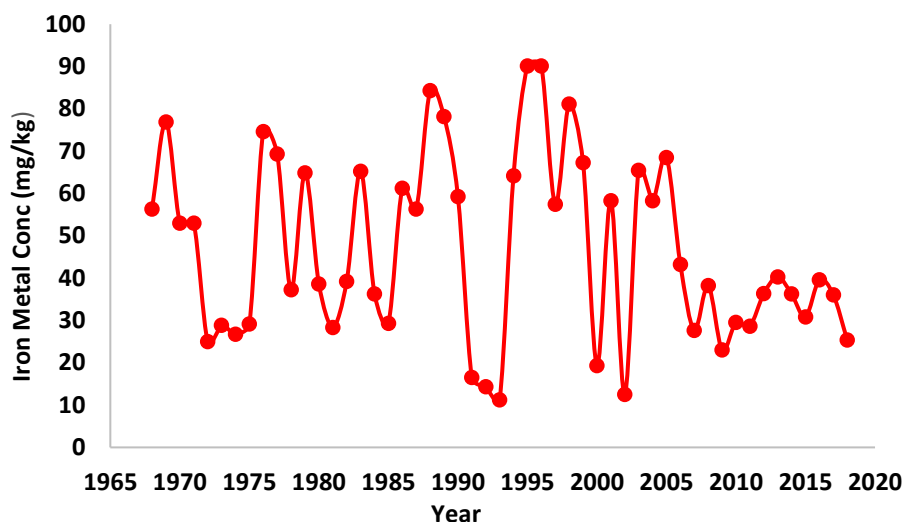
Figure 32: Iron Concentration at Tema Industrial Area

Comparison of Concentration in Trees at Haatso-Atomic and Tema Industrial Area within the Same Time Span

Similar concentration trend can be observed at both locations with Cu, Pb and Zn levels at Haatso-Atomic road being the highest for all years. These high concentrations of these heavy metals could be potentially credited to heavy traffic on the stretch of the road. One could also observe lower levels of pollutants from the industrial area which could potentially be attributed to the stern regulations and monitoring implemented by the environmental protection authority on industrial emissions as shown in Figure 33.

64
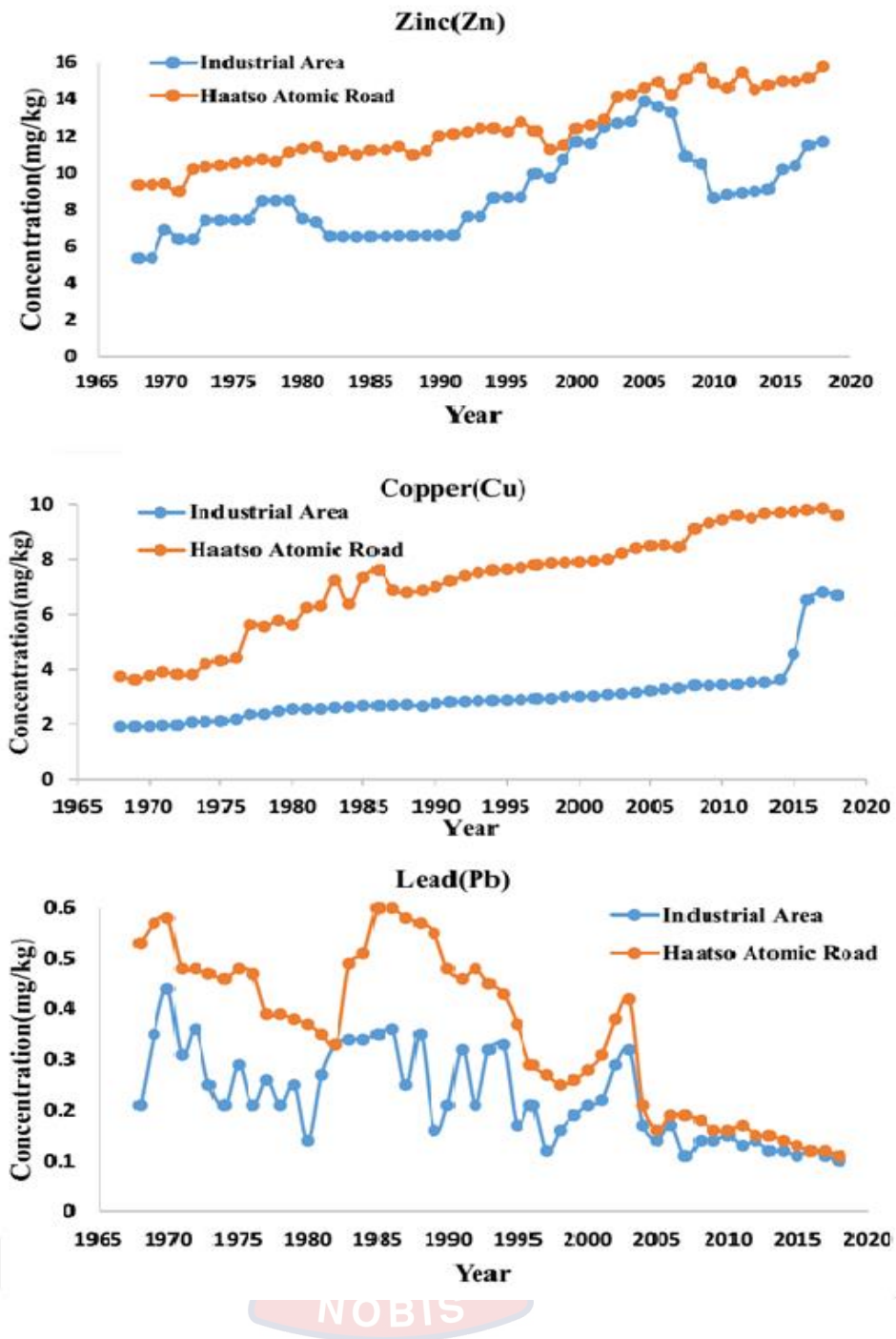
Figure 33: Comparison of Zn, Pb and Cu Concentration in Trees at Haatso-
        Atomic Road and Tema Industrial Area

Pearson Correlation at the Sampling Sites

Pearson correlation was performed to confirm whether there exists a growth relationship between the trees from the two locations as indicated in Figure 34.

65

Strong positive correlation was observed between growth of trees from Haatso-Atomic and Tema industrial Area with a correlation co-efficient of 0.853 which means, similar growth patterns could be concluded for the tree samples at both locations. This finding could also suggest the independence of the growth of the rings from the levels of pollutants in the environment as shown in Figure 34
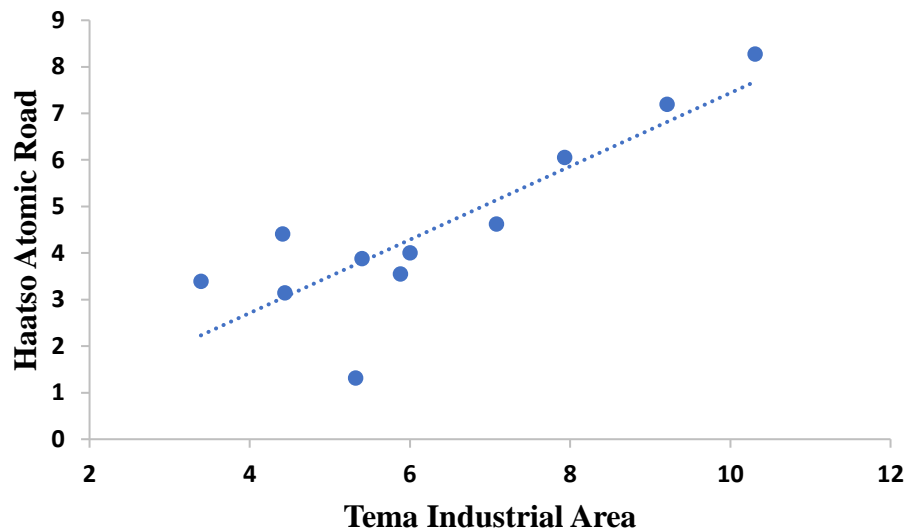
Figure 34: Pearson correlation for sample from Haatso Atomic and Tema Industrial Area

To confirm this statement, a correlation test was performed between growth rings width and the levels of pollutants recorded in the tree rings. This is presented in Table 2 for Haatso-Atomic road samples and Table 3 for Tema Industrial Area.

Table 2: Correlation Between Ring Width and Elemental Concentrations for Haatso Atomic Road

Heavy metal	Pearson correlation(r)
Copper	-0.18
Zinc	-0.22
Lead	0.22
Nickel	-0.21
Cadmium	-0.22
Manganese	-0.15

From Table 2, although there was negative correlation between the concentrations of (Cu, Zn, Ni, Cd and Mn) and the widths of growth rings, the correlation coefficients recorded were very low to make such a correlation significant.   The case was quite similar for Table 3, which illustrates the correlation between the concentrations of elements and the ring widths with the exception of a moderate negative correlation between growth widths and the levels of Zn in the atmosphere. A correlation coefficient of 0.56 was recorded. This means that for the tree at the industrial area, the levels of Zn could possibly have affected the growth trend of the rings.

Table 3. Correlation Between Ring Width and Elemental Concentrations for Tema Industrial Area

Heavy metal	Pearson correlation(r)
Copper	-0.26
Zinc	0.56
Lead	-0.25
Nickel	0.29
Cadmium	-0.06
Iron	0.10

67

Chapter summary

The results and discussion are summarized as follows;

The heavy metal from vehicular and industrial sources were Zn, Cu, Cd, Mn, Ni, Fe and Pb. Growth rates measured from tree rings were compared with precipitation data from the two sampling sites.

All the instruments passed the quality control/assurance tests that were carried out. The quality control/assurance procedure apply were core samples were collected at the breast height level to obtain the intrinsic properties in standing tree and also borer was sharpened and cleaned before coring the tree.

A total of 6 trees of Swietenia mahagoni were used. At both sampling sites, tree rings were counted, covering from 1957 to 2018 and 1968 to 2018. EDXRF spectrometer was used to investigate the presence of heavy metals in tree rings. It was observed that some of the heavy metals (Cd, Fe and Mn) were substantially higher than WHO guidelines. Cu, Zn, Pb, and Ni across the two sampling sites were below WHO maximum limit for heavy metals in plants.

The low levels of Pb concentrations recorded in this study confirmed the positive phase out of the use of leaded fuel. It was also observed that wet seasons correlate with high growth rate of trees while low precipitation seasons related to low or no growth rate of trees.

CHAPTER FIVE

SUMMARY, CONCLUSIONS AND RECOMMENDATIONS

Overview

In dendrochronology, the annual tree rings are used to determine the age of the tree by counting the number of rings. From the first ring, which is the pith and the center of the tree, to the last ring, the ring closest to the bark. The last ring represents the present year if the sample is collected during or after the growing season of that year. So, tree rings which is vital for the reconstruction of past climates was used. Swietenia mahagoni (Mahogany) tree which is over 50 years in age was chosen for this study because it produces annual growth rings. This study therefore determined the heavy metals pollution chronologies from vehicular and industrial emissions in the atmosphere using tree-rings as bio-indicators. Energy Dispersive X-ray Fluorescence (EDXRF) was utilized to determine the presence and concentration of the following heavy metals (Cu, Mn, Zn, Pb, Cd, Fe and Ni) in the tree rings sampled.

Summary

Air pollution monitoring was performed at Haatso-Atomic road and Tema industrial area using tree ring as bio indicator to determine pollutants in the air for a period of 50 years. A total of 6 trees of Swietenia mahagoni were used. At both sampling sites, tree rings were counted, covering from 1957 to 2018 and 1968 to 2018. EDXRF spectrometer was used to investigate the presence the following heavy metals (Cu, Mn, Zn, Pb, Cd, Fe and Ni). Concentration of copper, manganese, zinc, lead, cadmium, iron and nickel across the two sampling sites ranged from (1.92—9.84mg/kg), (2.58 – 5.49 mg/kg), (5.37 – 15.78mg/kg), (0.12—0.60 mg/kg), (0.01—0.09 mg/kg) (11.21—90.13 mg/kg) and (0.10 – 0.99 mg/kg) respectively.

It was observed that some of the heavy metals (Cd, Fe and Mn) were substantially higher than WHO guidelines which could attributed to pollution from the wear and tear of brake pads and other automobile parts as well as additive in fuels. Cu, Zn, Pb, and Ni across the two sampling sites were below WHO maximum limit for heavy metals in plants. The low levels of Pb concentrations recorded in this study confirmed the positive phase out of the use of leaded fuel. It was also observed that wet seasons correlate with high growth rate of trees while low precipitation seasons related to low or no growth rate of trees.

Conclusions

Tree rings have been used as proxies to establish pollution chronologies from vehicular and industrial emissions into the atmosphere for a period spanning from 1957 to 2018 and 1968 to 2018. Pollutant from vehicular and industrial emissions, which contributes to the increase of Zinc (Zn), Nickel (Ni), Copper (Cu), Lead (Pb), Manganese (Mn) Iron (Fe) and Cadmium (Cd) in the atmosphere have been measured in tree rings for a period of over 50 years. There is a worrying trend observed for some of these heavy metals (Zn, Ni, Cu, Cd and Mn) as the levels of these metals have been increasing steadily over the past decades. This raises lots of concerns because if this trend is not halted, this can affect the whole ecosystem. Some heavy metals (Mn, Cd and Fe) recorded (2.58 – 5.49 mg/kg), (0.01—0.09 mg/kg) and (11.21—90.13 mg/kg) were substantially higher than WHO guideline limits in plants.

Tree growth rings have been related to annual rain fall patterns. In this study, high precipitation (wet seasons) has been linked to increased growth of tree rings. No or stunt growth of tree rings has also been linked to harsh environmental conditions such as drought (dry seasons). There was negative

correlation between the concentrations of (Cu, Ni, Cd, Pb and Mn) and for the widths growth rings, the correlation coefficients recorded were very low (-0.18, -0.21, -0.22, 0.22 and -0.15) to make such a correlation significant.

Recommendations

In   the light of the above findings the following recommendations were made

1.   For Environmental Protection Agency (EPA):

    a.   The observed concentrations of some heavy metals are worrying and there is the need to take some mitigation measures to reduce the levels.

    b.   Stricter EPA guidelines are required to regulate importation of over-aged second-hand vehicles.

2. For Further Study:

    a.   More tree that produce annual ring need to be studied to broaden the scope   of the work.

    b. Computer model could be developed to predict future pollution levels.

71

REFERENCES

Aboh, I. J. K., Ofosu, G. K., Hopke, P. K., & Bamford, S. A. (2012). Characterization of fine particulate sources at Ashaiman in Greater Accra, Ghana. *Atmospheric Pollution Research,* 3, 301-310.

Aboh, I., (2000). Characterization and sources of air particulate matter at Kwabenya, near Accra, Ghana. Published doctoral thesis, University of Ghana.

Abu-Allaban, M., Gillies, J. A., Gertler, A. W., Clayton, R., Proffitt. D. & Tailpipe, D. (2003). Resuspended road dust, and brake-wear emission factors from on-road vehicles. *Atmospheric Environment,* 37, 5283- 5293.

Agyemang, B. W. K., Tutu, B, D., & Asiamah, H. (2007). Ghana vehicular emission report, Accra, *Ghana. Environmental Protection Agency, Accra.*

Akumu, J., (2014). Air quality in African cities, UNEP. Retrieved from http://unep.org/transport.

Agency for Toxic Substances and Disease Registry. (2007). Toxicological profile for lead. Public Health Service. Atlanta, USA: ATSDR.

Agency for Toxic Substances and Disease Registry. (2004). Toxicological profile for copper. Public Health Service. Atlanta, USA: ATSDR.

Agency for Toxic Substances and Disease Registry. (2012). Toxicological profile for cadmium. Public Health Service. Atlanta, USA: ATSDR.

Awan, M. A., Ahmed, S. H., Aslam, M. R., & Qazi, I. A. (2011). Determination of total suspended particulate matter and heavy metals in ambient air of four cities in Pakistan. *Journal of Energy and Environment,* 2 (2), 128-132.

Batterman, S., Zhang, K., & Kononowech, R. (2013). Prediction and analysis of near-road concentrations using a reduced-form emission/dispersion model. *Environmental Health*, 9, 29.

Bargagli, R., (1998). Trace Element in terrestrial plants. An ecophysiological approach to biomonitoring and bio-recovery. *Springer Verlag,* Berlin, New York*:* pp. 324.

Belis, C., Karagulian, F., Larsen, B., & Hopke, P. (2013). Critical review and meta-analysis of ambient particulate matter source apportionment using receptor models in Europe. *Atmospheric Environment*, 69, 94–108.

Benjamin, A., & Ayatulai-Abdul, M. (2018). Assessment of inhalable particular matter (PM) associated with a cement factory in Tema, Ghana. *American Journal of Environmental engineering.* 8(5), 167-173.

Boni, C., Caridi, A., Cereda, E., & Marcazzan, G. B. (1990). A PIXE-PIGE setup for the analysis of thin samples. Nuclear Instruments and Methods in Physics Research Section: Beam Interactions with Materials and Atoms, 47(2),133–142.

Braga, C. F., Teixeira, E. C., Meira, L., Wiegand, F., Yoneama, M. L., & Dias, J. F. (2005). Elemental composition of PM_{10} and $PM_{2.5}$ in urban environment in South Brazil. *Atmospheric Environment,* 39, 1801-1815.

Brouwer, P. N. (2006). Theory of XRF. PANalytical BV, Netherlands.

Cao, J., Lee, S., Zheng, X., Ho, K., Zhang, X., Guo, H., Chow, J. C., & Wang, H. (2003). Characterization of dust storms to Hong Kong in April 1998. *Water, Air and Soil Pollution*, 3(2), 213–229.

Celik, A., Kartal, A., Akdogan, A., & Kaska, Y, (1995) Determining the heavy metal pollution in Denizli (Turkey) by using Robinio pseudo-acacia. *Environmental International*, 31, 105-112, 19.

Chang, Y., Lee, H., & Huang, J. (2016). Risk factors and outcome analysis in children with carbon monoxide poisoning. Pediatrics and Neonatology, 1–7.

Cheung, C. S. & Kong, H. (2002). Better air quality: Proceedings of the regional workshop on better air quality in Asian and Pacific Rim cities, 16-18 December 2002, Hong Kong. Department of Civil and Structural Engineering, the Hong Kong Polytechnic University.

Chiarenzelli, J. R., Aspler, L. B., Dunn, C., Cousens, B., Ozarko, D. L., & Powis, K. B. (2001). Multi-element and rare earth element composition of lichens, mosses, and vascular plants from the Central Barrenlands, Nunavut, Canada. *Applied Geochem,* 16, 245-270.

Cocozza, C., Ravera, S., Cherubini, P., Lombardi, F., Marchetti, M., & Tognetti, R. (2016). Integrated biomonitoring of airborne pollutants over space and time using tree rings, bark, leaves and epiphytic lichens. *Urban for Green*. 17, 177-191.

Danek, M., Bell, T., & Laroque, C. P. (2015). Some considerations in the reconstruction of lead levels using laser ablation: Lessons from the design stage of dendrochemistry study, St. John's, Canada. *Geochronometria*, 42, 217-23.

Dionisio, K. L., Arku, R. E., Hughes, A. F., Vallarino, J., Carmichael, H., Spengler, J. D., Agyei, M, S., & Ezzati, M. (2010). Air pollution in

74

Accra neighborhoods: Spatial, socioeconomic, and temporal patterns. *Environmental Science and Technology,* 44, 2270–2276.

Elena, C., Daniela, T. A., & Anca, F. G. (2018). Transport infrastructure development, public performance and long-run economic growth; A case study for the Eu-28 countries. *Sustainability*, 11(1), 67.

European Commission. (2001). Working group on arsenic, cadmium and nickel compounds: Ambient air pollution by As, Cd and Ni compounds position. Office for Official Publications of the European Communities Luxembourg.

Fabretti, J. F., Sauret, N., Gal, J. F., Maria, P. C., & Scharer, U. (2009). Elemental characterization and source identification of $PM_{2.5}$ using positive matrix factorization: The Malraux road tunnel, nice, France. *Atmospheric Research*, 94(2), 320–329.

Fritts, H. C., (2012). Tree rings and climate. Elsevier. pp. 15

Garg, B. D., Cadle, S. H., Mulawa, P. A., Groblicki, P. J., Aroo, C., & Parr, G. A. (2000). Brake wear particulate matter emissions. *Environment. Science Technology.* 34, 4463-4469.

Garman, E. F., & Grime, G. W. (2005). Elemental analysis of proteins by micropixe. Progress in biophysics and molecular biology, 89(2),173–205.

Gerward, L., (1993). X-ray attenuation coefficients: Current state of knowledge and availability. *Radiation Physics-Chemical*, 41**,** 783-789.

Ghana Automobile Market (2019). Ghana's automobile market - growth, trends, and forecast 2020 – 2025 (Industry Report of Automobile-Industry in Ghana). https://www.mordorintelligence.com/analysis of automobile in ghana.

Global Environment Facility. (2007). Ghana urban transport project. Global Environment Facility. http://www.theGEF.org. (Accessed on 11/12/2012).

Guthrie, J. M., (2012). Overview of X-ray Fluorescence. University of Missouri Research Reactor.

Gurol, A., (2008). X-ray fluorescence spectrometry. *Applied Radiation and Isotopes,* 66(3), 372–376.

Hopke P. K., Ito, K., Mar, T., Christensen, W. F., Eatough, D. J., Henry, R. C., Kim, E., Laden, F., Lall, R., Larson, T. V., Liu, H., Neas, L., Pinto, J., Stölzel, M., Suh, H., Paatero, P., & Thurston, G. D. (2006). PM source apportionment and health effects. *Journal of Exposure Science Environment*, 16, 275–286.

Huang, S., & Conte, M. (2009). Source/process apportionment of major and trace elements in sinking particles in the Sargasso Sea. *Geochemical ET Cosmochimica Acta,* 73(1), 65–90.

Hughes, A. F., (2014). Characterization and source apportionment of airborne particulate matter in some urban neighborhoods of Accra, Ghana. Published doctoral thesis, University of Ghana.

Jex, D., Hill, M., & Mangelson, N. (1990). Proton induced x-ray emission of spherical particles: Corrections for x-ray attenuation. Nuclear Instruments and Methods in Physics Research Section B: Beam Interactions with Materials and Atoms, 49(4), 141–145.

Johansson, S. A., Campbell, J. L., & Malmqvist, K. G. (1995). Particle induced X-ray emission spectrometry (PIXE). Volume 133. New Jersey, John Wiley & Sons Inc: USA.

Jones, S., Tefe, M., Zephaniah, S., Tedla, E., Appiah-Opoku, S., & Walsh, J. (2016). Public transport and health outcomes in rural sub-Saharan Africa - A synthesis of professional opinion. *Journal of Transport and Health*, 3(2), 211–219.

Kadiyala, A., & Kumar, A. (2013). Quantification of in-vehicle gaseous contaminants of carbon dioxide and carbon monoxide under varying climatic conditions. Air Quality, *Atmosphere and Health*, 6(1), 215–224.

Kam, W., Liacos, J. W., Schauer, J. J., Delfino, R. J. & Sioutas, C. (2012). On-road emission factors of PM pollutants for light-duty vehicles (LDVs) based on urban street driving conditions. *Atmospheric Environment*, 61, 378-386.

Kathie, L. D., Raphael, E., Allison, F. H., & Agyei, M. S. (2010). Air pollution in Accra neighborhoods: Spatial, socio-economic and temporal patterns. *Environment Science and Technology*, 44(7), 2270-2276.

Kojima, M., & Lovei, M. (2001). Urban air quality management: Coordinating transport, environment, and energy policies in developing countries. (World Bank Technical Paper No. 508), Washington DC, pp. 56

Kothai, P., Saradhi, I. V., Prathibha, P., Hopke, P. K., Pandit, G. G., & Puranik, V. D. (2008). Source apportionment of coarse and fine particulate matter at Navi Mumbai, India. *Aerosol and Air Quality Research*, 8(4), 423–436.

Krzyzanowski, M., & Cohen, A. (2008). *Update of WHO air quality guidelines*. Air Quality. Atmosphere and Health, 1(1); 7–13.

Kupiainen, K., (2007). Road dust from pavement wear and traction sanding. *Monographs of the Boreal Environment Research*. 2, 50.

Lannefors, H., Hansson, H. C., & Granat, L. (1983). Background aerosol composition in southern Sweden fourteen micro and macro constituents measured in seven particle size intervals at one site during one year. *Atmospheric Environment*. 17(1), 87–101.

Leili, M., Naddafi, K., Nabizadeh, R., Yunesian, M., & Mesdaghinia, A. (2008). The study of TSP and PM_{10} concentration and their heavy metal content in central area of Tehran, Iran. *Air Quality Atmospheric Health*, 1, 159–166.

Lee, D. S., Pitari, G., Grewe, V., Gierens, K., Penner, J. E., Petzold, A., Prather, M. J., Schumann, U., Bais, A., Berntsen, T., & Iachetti, D. (2010). In atmospheric environment transport impacts on atmosphere and climate*: The ATTICA Assessment Report,* 44(37), 4678-4734.

Luke, D., (2011). A review of commuter exposure to ultrafine particles and its health effects international laboratory for air quality and health. Queensland University of Technology, Brisbane, Australia: *Institute of Health and Biomedical Inn,* 45, 2611–2622

Markert, B. A., Breure, A. M., & Zechmeister, H. G. (2003). Definitions, strategies, and principles for bioindication/biomonitoring of the environment. *Elsevier Science Ltd*, 5-69.

Markert, B. A., (2003). Definitions, strategies and principles for biomonitoring of the environment. *Elsevier Science Ltd,* 3-39.

Markert, B., Oehlann, J., & Roth, M. (1997). General aspects of heavy metal monitoring by plants and animals. ACS Symposium Series, *American Chemical Society,* 654, 19-29.

Md-Tanvir, H. M., Emadu, H., & Rajada, K. (2017). Heavy metal contamination in agricultural soil at DEPZA, Bangladesh. *Environment and Ecology Research,* 5(7), 510-516.

Nave, C. R., (2013). Characteristic X-rays. Hyper Physics.

Nastasi, M., Mayer, J. W., & Wang, Y. (2015). Ion beam analysis – fundamentals and applications. CRC Press.

Nerquaye-Tetteh, E., (2009). Urban air quality monitoring programme in Accra. Environmental Protection Agency, Accra, Ghana. Available: http://www.unep.org/urbanenvironment/PDFs/BAQ09 ghanacasestudy.pdf (Accessed 2/10/2013).

Nriagu, J., (2007). Zinc toxicity in humans. School of Public Health, University of Michigan.

Odabasi, M., Falay, E., Tuna, G., Altiok, H., Kara, M., Dumanoglu, Y., Bayram, A., Tolunay, D., & Elbir, T. (2015). Biomonitoring the spatial and historical variations of persistent organic pollutants (POPs) in an industrial region. *Environmental Science Technology,* 49, 2105-2114

Ondracek, J., Schwarz, J., Zdímal, V., Andelova, L., Vodicka, P., Bizek, V., Tsai, C. J., Chen, S. C., & Smolik, J. (2011). Contribution of the road traffic to air pollution in the Prague city (busy speedway and suburban crossroads). *Atmospheric Environment*, 45, 5090–5100.

Opazo, C. M., Greenough, M. A., & Bush, A. I. (2014). Copper from neurotransmission to neuroproteostasis. *Front Aging Neuroscience.* Vol.6, Article 143.

Paatero, P., & Tapper, U. (1994). Positive matrix factorization: A nonnegative factor model with optimal utilization of error estimates of data values. *Environmetrics*, 5(2), 111–126.

Padilla, K. L., & Anderson K. A. (2002). Trace element concentration in tree-rings biomonitoring centuries of environmental change. *Chemosphere. 49(6),575-85.*

Palmieri, F., Neri, R., Benco, C., & Serracca, L. (2016). Lichens and moss as bioindicators and bioaccumulator in air pollution monitoring. Air pollution in formation system. *Journal of Environment*, 75, 1260.

Pdamo, P., Giordano, S., Vingiani, S., & Violante, P. (2003). Trace element accumulation by moss and lichen exposed in bags in the city of Naples (Italy). *Environmental Pollution.* 122, 91-10.

Perone, A., Cocozza, C., Cherubini, P., Bachmann, O., Guillong, M., Lasserre, B., Marchetti, M., & Tognetti, R. (2018). Oak tree-rings record spatial-temporal pollution trends from different sources in Terni (Central Italy). *Environmental Pollution,* 233, 278-289.

Poikolainen, J., (2004). Mosses, epiphytic lichens and tree bark as biomonitors for air pollutants – specifically for heavy metals in regional surveys. The Finnish Forest Research Institute, Muhos Research Station.

Popescu, C. G., (2011). Relation between vehicle traffic and heavy metals content from the particulate matters. *Romanian Reports in Physics*, 63(2), 471–482.

Pongkiatkul, P., & Oanh, N. T. K. (2012). Receptor modeling for air pollution source apportionment study. Integrated Air Quality Management: Asian Case Studies, 63.

Prudêncio, M., I. Gouveia, M. A., Freitas, M. C., Chaves, I., & Marques, A. P. (2000). Soil versus lichen analysis on elemental dispersion studies (North of Portugal). Proc. Inter. Workshop: BioMAP, 21-24 September 1997, IAEA-TECDOC-1152. International Atomic Energy Agency, Vienna: 91-99.

Pumijumnong, N., Eckstein, D., & Park, W. K. (2001). Teak tree-ring chronologies in Myanmar first attempt. *International Palaeobotanist,* 50, 35–40.

Rasmussen, L., (1978). Element content of epiphytic hypnum cupressiforme related to element content of the bark of different species of phorophytes. *Lindbergia,* 4, 209-218.

Razos, P., & Christides, A. (2010). An investigation on heavy metals in an industrial area in Greece. *International Journal of Environmental Research,* 4(4), 785-794.

Rühiling, A., (1994). Atmospheric heavy metal deposition in Europe-estimations based on moss analysis. Nordic Council of Ministers, (ed.) AKA Print, A/S Arhus. pp.9

Safo-Adu, G., Ofosu, F. G., Carboo, D., & Armah, Y. S. (2014). Heavy metals and black carbon assessment of PM$_{10}$ particulates along Accra-Tema highway in Ghana. *International Journal of Science and Technology*, 8, 467-474.

Schauer, J. J., Lough, G. C., Shafer, M. M., Christensen, W. F., Arndt, M. F., De-Minter, J. T., & Park, J. S. (2006). Characterization of metals emitted from motor vehicles. (Research Report No 133). Health Effects Institute, Boston, MA.

Schrank, D., & Lomax T. (2008). 2007 urban mobility report. (Accessed 22/03/2008).

Schwarze, P., Qvrevik, J., Lag, M., Refsnes, M., Nafstad, P., Hetland, R., & Dybing, E. (2006). Particulate matter properties and health effects: consistency of epidemiological and toxicological studies. *Human and Experimental Toxicology*, 25(10), 559–579.

Sitko, R., Zawisza, B., & Malicka, E. (2009). Energy-dispersive X-ray fluorescence spectrometer for analysis of conventional and micro-samples: preliminary assessment. Spectrochimica Acta Part B: *Atomic Spectroscopy,* 64(5), 436–441.

Siyan, P., Eremiokhale, R. & Makwe, E. (2015). The impact of road transportation infrastructure on economic growth in Nigeria. *International Journal of Management and Commerce Innovations.* 3(1): 673-680.

Sloof, J. E., (1993). Environmental lichenoloy: biomoniroing trace element air pollution. University of Technology, Delft, Netherlands: ISBN 90-73861-12-8.

Speer, J., (2010). Fundamentals of tree-ring research. Tucson: University of Arizona Press.

Szczepaniak, K., & Biziuk, M. (2003). Aspect of the biomonitoring studies using mosses and lichen as indicators of metal pollution. *Environmental Research*, 93(3), 221-30.

Talebi, S. M., & Tavakoli-Ghinani, T. (2008). Levels of pm_{10} and its chemical composition in the atmosphere of the city of Isfahan. *Iranian Journal of Chemical Engineering,* 5(3), 62-67.

Tema Metropolitan Archived. (2010). At the way back machine. Ghana Districts.com. Retrieved 9/03/ 2013.

Thorpe, A., & Harrison, R. M. (2008). Sources and properties of non-exhaust particulate matter from road traffic. *Science Total of the Environment,* 400(1-3), 270–282.

Tong, S., Schirnding, Y. E. V., & Prapamontol, T. (2000). Environmental lead exposure: a public health problem of global dimensions. *Bulletin of the World Health Organization,* 78(9), 1068-1077.

Tyagi, V., Gurjar, B. R., Joshi, N., & Kumar, P. (2012). PM_{10} and heavy metals in sub-urban and rural atmospheric environments of northern India. *ASCE Journal of Hazardous, Toxic and Radioactive Waste,* 16, 175-182.

United Nations Environment Program (UNEP) (2010). Urban air pollution. http://www.unep.org/urban_environment/issues/urban_air.asp. (Accessed 14/06 /2013).

Vardoulakis, S., Fisher, B. E. A., Pericleous, K., & Gonzalez-Flesca, N. (2003). Modelling air quality in street canyons: a review. *Atmospheric Environment*, 37, 155-182.

Vecchi, R., Marcazzan, G., & Valli, G. (2007). A study on nighttime-daytime PM_{10} concentration and elemental composition in relation to atmospheric dispersion in the urban area of Milan. *Atmospheric Environment,* 41, 2136 –2144.

Wahlin, P., Berkowicz, R., & Palmgren, F. (2006). Characterization of traffic generated particulate matter in Copenhagen. *Atmospheric Environment,* 40 (12), 2151 – 2159.

Wajid, R., Akif, Z., Nayyara, N., & Mohsan, N. (2008). Heavy metal pollution assessment in various industries of Pakistan. *Environment Geology*, 55, 353–358.

Wakisaka, T., Morita, N., Wakasa, M., Terada, S., Nishihagi, K., & Taniguchi, K. (1996). Development of energy dispersive X-ray fluorescence spectrometer with monochromatic excitation for the direct determination of trace elements in organic matrices. *Bunseki Kagaku,* 45(10), 933–939.

Watson, J., Chow, J., & Frazier, C. (1999). X-ray fluorescence analysis of ambient air samples. Elemental analysis of airborne particles, 1, 67–96.

Wittke, J. H., (2013). The origin of characteristic X-ray. Retrieved (18/06/ 2013).

Wolterbeek, H. T., Bode, P., & Verburg, T. G. (1996). Assessing the quality of biomonitoring via signal-to-noise ratio analysis. *Science of the Total Environment*, 180, 107-116.

World Health Organization. (2016). Ghana Life Expectancy. Ghana: WHO statistical profile, 1–3. Retrieved from http://www.who.int/ countries/gha/en. WHO.

Ya-Fen, W., (2003). Emissions of fuel metals content from a diesel vehicle engine. *Atmospheric Environment*, 37(33), 4637-4643.

Yongjie, Y., Yuesi, W., Tianxue, W., Wei, L., Ya'nan, Z., & Liang, L. (2009). Elemental composition of $PM_{2.5}$ and PM_{10} at Mount Gongga in China during 2006. *Atmospheric Research*, 93, 801–810.

Yorke, C. K. A., & Omotosho, J. B. (2010). Rainfall variability in Ghana during 1961- 2005. *Journal of Ghana Science Association,* 12, 1.

Zaigham, H., Zubair, A., & Khalid, U. K. (2012). Civic pollution and its effect on water quality of River Toi at district Kohat, NWFP. *Research Journal of Environmental and Earth Sciences*, 4, 5.

Zhang, Y. X., Quraishi, T. & Schauer, J. J. (2008). Daily variations in sources of carbonaceous aerosol in Lahore, Pakistan during a high pollution spring episode. *Aerosol Air Quality Research*, 8,130–146.

APPENDICES

Appendix 1

HEAVY METAL CONCENTRATIONS AT HAATSO-ATOMIC ROAD

Heavy Metal Concentrations in (mg/kg) at Haatso-Atomic Road						
Year	Elemental concentrations (mg/kg)					
	Cu	Zn	Pb	Mn	Ni	Cd
2018	9.62	15.78	0.11	5.94	0.99	0.09
2017	9.86	15.17	0.12	5.86	0.97	0.09
2016	9.81	14.98	0.12	5.47	0.95	0.08
2015	9.75	14.99	0.13	4.68	0.97	0.07
2014	9.71	14.78	0.14	4.45	0.97	0.07
2013	9.69	14.52	0.15	4.42	0.96	0.07
2012	9.52	15.46	0.15	4.49	0.89	0.07
2011	9.62	14.62	0.17	4.61	0.87	0.06
2010	9.45	14.89	0.16	4.01	0.85	0.06
2009	9.34	15.71	0.16	4.12	0.85	0.06
2008	9.12	15.12	0.18	5.01	0.84	0.05
2007	8.46	14.25	0.19	4.01	0.83	0.05
2006	8.53	14.94	0.19	4.11	0.81	0.05
2005	8.50	14.63	0.16	4.01	0.82	0.05
2004	8.42	14.25	0.21	4.35	0.80	0.05
2003	8.23	14.14	0.23	4.58	0.78	0.05
2002	8.01	12.91	0.28	4.49	0.77	0.05
2001	7.95	12.61	0.27	4.91	0.79	0.05
2000	7.91	12.41	0.28	4.44	0.78	0.05
1999	7.89	11.51	0.26	4.44	0.78	0.04

1998	7.88	11.28	0.25	4.32	0.77	0.04
1997	7.81	12.27	0.27	4.45	0.76	0.04
1996	7.71	12.77	0.29	4.41	0.74	0.04
1995	7.65	12.23	0.37	4.71	0.72	0.03
1994	7.61	12.42	0.43	4.61	0.71	0.03
1993	7.53	12.42	0.45	4.61	0.69	0.03
1992	7.42	12.21	0.48	4.68	0.68	0.04
1991	7.23	12.11	0.46	3.99	0.68	0.05
1990	7.01	12.00	0.48	4.62	0.66	0.04
1989	6.88	11.21	0.55	3.99	0.65	0.04
1988	6.81	10.99	0.57	3.98	0.61	0.04
1987	6.89	11.45	0.58	4.58	0.59	0.03
1986	7.61	11.26	0.60	4.21	0.59	0.03
1985	7.35	11.24	0.60	4.66	0.58	0.03
1984	6.38	10.99	0.51	4.55	0.55	0.03
1983	7.25	11.21	0.49	4.78	0.53	0.03
1982	6.32	10.88	0.40	4.42	0.51	0.02
1981	6.25	11.42	0.35	4.31	0.48	0.03
1980	5.62	11.32	0.37	4.11	0.46	0.03
1979	5.78	11.12	0.38	3.62	0.41	0.03
1978	5.56	10.62	0.39	3.51	0.39	0.02
1977	5.62	10.74	0.39	3.65	0.38	0.02
1976	4.42	10.65	0.47	3.56	0.36	0.02
1975	4.32	10.54	0.48	3.57	0.33	0.03
1974	4.21	10.41	0.46	3.47	0.31	0.04
1973	3.81	10.34	0.47	3.43	0.28	0.04
1972	3.82	10.22	0.48	3.51	0.25	0.03
1971	3.91	8.99	0.48	3.45	0.24	0.03
1970	3.78	9.42	0.58	3.32	0.24	0.03
1969	3.63	9.36	0.57	3.18	0.22	0.02

1968	3.75	9.35	0.53	2.98	0.23	0.03
1967	3.61	9.41	0.51	2.99	0.21	0.03
1966	3.52	9.23	0.49	3.68	0.18	0.03
1965	3.34	8.76	0.46	3.65	0.19	0.02
1964	3.23	8.99	0.43	3.63	0.19	0.02
1963	3.16	8.71	0.39	3.65	0.17	0.02
1962	3.36	8.64	0.41	3.31	0.15	0.02
1961	3.26	8.52	0.51	2.91	0.13	0.03
1960	3.32	8.42	0.42	2.65	0.14	0.02
1959	3.45	8.25	0.45	2.68	0.12	0.01
1958	3.24	8.23	0.45	2.68	0.10	0.01
1957	3.15	8.18	0.41	2.58	0.11	0.01
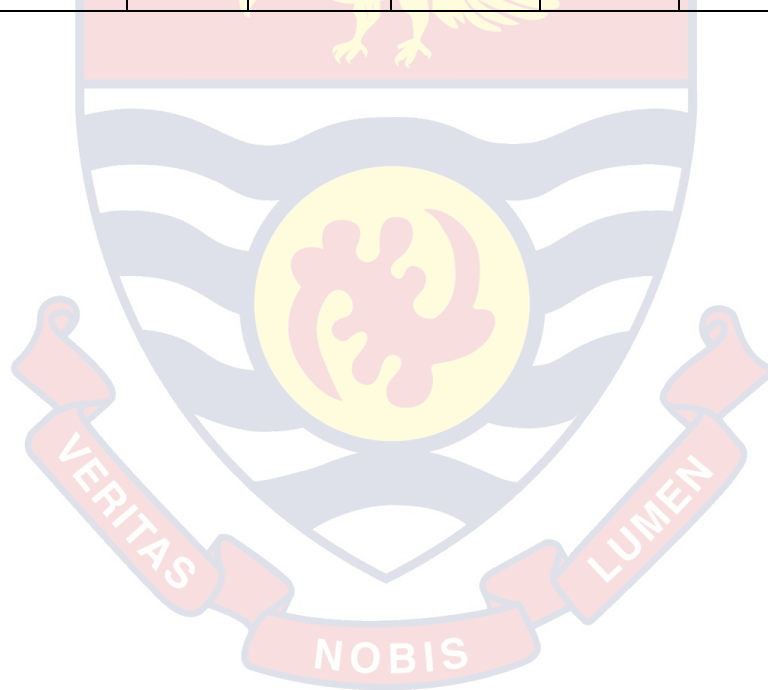
Appendix 2

HEAVY METAL CONCENTRATIONS AT TEMA INDUSTRIAL AREA

Heavy Metal Concentrations in (mg/kg) at Tema Industrial Area						
Year	Elemental concentrations (mg/kg)					
	Cu	Pb	Zn	Fe	Ni	Cd
2018	6.70	0.10	11.70	25.39	1.16	0.01
2017	6.82	0.11	11.50	36.07	2.35	0.02
2016	6.53	0.12	10.40	39.62	1.91	0.02
2015	4.56	0.11	10.20	30.83	1.78	0.01
2014	3.64	0.12	9.11	36.25	2.32	0.03
2013	3.53	0.12	9.00	40.31	2.14	0.02
2012	3.53	0.14	8.91	36.34	1.14	0.01
2011	3.46	0.13	8.82	28.65	1.18	0.02
2010	3.45	0.15	8.64	29.56	1.97	0.01
2009	3.42	0.14	10.50	23.06	1.18	0.01
2008	3.43	0.14	10.90	38.25	1.20	0.03
2007	3.32	0.11	13.30	27.68	1.51	0.04
2006	3.29	0.17	13.60	43.25	2.54	0.02
2005	3.22	0.14	13.90	68.52	2.99	0.04
2004	3.16	0.17	12.80	58.32	3.59	0.07
2003	3.11	0.32	12.70	65.52	5.31	0.07
2002	3.08	0.29	12.50	12.52	6.26	0.08
2001	3.03	0.22	11.60	58.32	8.63	0.05
2000	3.02	0.21	11.70	19.35	7.62	0.04
1999	3.01	0.19	10.73	67.32	7.36	0.01
1998	2.93	0.16	9.72	81.14	2.89	0.03

1997	2.93	0.12	9.96	57.48	2.77	0.03
1996	2.89	0.21	8.68	90.13	4.34	0.04
1995	2.88	0.17	8.67	90.13	4.34	0.04
1994	2.87	0.33	8.65	64.22	3.24	0.03
1993	2.86	0.32	7.64	11.21	6.85	0.01
1992	2.83	0.21	7.63	14.35	5.68	0.02
1991	2.82	0.32	6.61	16.52	7.62	0.04
1990	2.76	0.21	6.62	59.31	6.82	0.03
1989	2.66	0.16	6.60	78.21	7.89	0.02
1988	2.72	0.35	6.59	84.32	8.68	0.05
1987	2.70	0.25	6.58	56.32	6.38	0.03
1986	2.68	0.36	6.56	61.25	8.63	0.04
1985	2.68	0.35	6.54	29.32	8.62	0.01
1984	2.63	0.34	6.53	36.32	5.62	0.02
1983	2.61	0.34	6.55	65.25	6.32	0.03
1982	2.56	0.33	6.56	39.23	8.65	0.01
1981	2.56	0.27	7.33	28.36	7.35	0.01
1980	2.56	0.14	7.52	38.62	6.87	0.04
1979	2.48	0.25	8.51	64.85	5.36	0.05
1978	2.37	0.21	8.49	37.25	8.25	0.02
1977	2.36	0.26	8.48	69.34	6.94	0.06
1976	2.18	0.21	7.46	74.62	9.65	0.04
1975	2.12	0.29	7.45	29.15	9.52	0.05
1974	2.10	0.21	7.43	26.75	9.82	0.05
1973	2.08	0.25	7.42	28.84	2.45	0.03
1972	1.97	0.36	6.39	25.04	1.12	0.01
1971	1.96	0.31	6.40	53.02	2.42	0.02
1970	1.93	0.44	6.91	53.04	2.49	0.02
1969	1.92	0.35	5.38	76.92	3.15	0.02
1968	1.92	0.21	5.37	56.32	6.25	0.01

Appendix 3

TREE RING WIDTH IN (mm) FOR AVERAGE OF 5 YEARS

Haatso-Atomic Road		Tema Industrial Area	
Average Year	Average Ring Width	Average Year	Average Ring Width
1959	3.63	1969	9.21
1964	4.43	1974	7.08
1969	7.19	1979	10.31
1974	4.62	1984	7.93
1979	8.27	1989	6.00
1984	6.05	1994	3.39
1989	4.00	1999	4.41
1994	3.39	2004	5.40
1999	4.41	2009	5.88
2004	3.88	2014	4.44
2009	3.55	2018	5.32
2014	3.14		
2018	1.31		

Appendix 4

TREE RING WIDTH IN (mm) AT HAATSO-ATOMIC ROAD

Year	Ring width	Year	Ring width
2018	0.000	1987	0.866
2017	2.639	1986	0.967
2016	6.215	1985	6.074
2015	2.577	1984	5.021
2014	1.01	1983	13.325
2013	1.76	1982	4.879
2012	4.185	1981	7.669
2011	9.936	1980	4.285
2010	0.643	1979	17.652
2009	0.576	1978	8.084
2008	3.491	1977	3.684
2007	3.107	1976	7.169
2006	2.11	1975	9.708
2005	1.958	1974	1.984
2004	6.925	1973	1.320
2003	2.318	1972	2.923
2002	6.133	1971	1.367
2001	3.151	1970	10.513
2000	4.01	1969	2.149
1999	7.301	1968	18.552
1998	5.901	1967	3.375
1997	1.688	1966	4.061
1996	0.757	1965	8.303
1995	5.423	1964	4.768
1994	4.12	1963	3.045
1993	4.574	1962	1.984
1992	2.102	1961	5.015
1991	8.293	1960	2.695
1990	1.452	1959	3.754
1989	3.752	1958	4.492
1988	5.674	1957	2.221

Appendix 5

RAINFALL DATA FORM METEOROLOGICAL STATIONS FOR TEMA

AND ACCRA

Tema		Accra	
Year	Rainfall(mm)	Year	Rainfall(mm)
1968	138.03	1957	62.93
1969	54.19	1958	58.98
1970	57.58	1959	86.45
1971	75.27	1960	58.71
1972	68.48	1961	81.29
1973	70.95	1962	102.56
1974	72.82	1963	112.56
1975	58.44	1964	72.19
1976	46.72	1965	87.84
1977	27.45	1966	47.23
1978	31.56	1967	67.68
1979	73.18	1968	117.73
1980	75.11	1969	55.62
1981	61.84	1970	74.51
1982	61.81	1971	76.59
1983	30.05	1972	67.01
1984	38.44	1973	81.74
1985	45.29	1974	19.63
1986	30.67	1975	74.31
1987	57.78	1976	45.80
1988	60.83	1977	31.09
1989	51.32	1978	44.78
1990	45.24	1979	76.45
1991	63.82	1980	82.74
1992	38.16	1981	55.81
1993	42.72	1982	64.50
1994	41.76	1983	77.76
1995	74.53	1984	58.76
1996	79.57	1985	56.72
1997	27.91	1986	45.43
1998	107.9	1987	53.32
1999	42.93	1988	82.41
2000	34.74	1989	54.73

2001	61.73	1990	47.33
2002	70.41	1991	85.03
2003	59.87	1992	46.42
2004	33.92	1993	40.73
2005	50.90	1994	45.66
2006	56.26	1995	85.82
2007	86.92	1996	59.71
2008	55.14	1997	101.96
2009	52.83	1998	42.80
2010	78.86	1999	53.48
2011	74.39	2000	42.68
2012	56.07	2001	66.78
2013	40.38	2002	74.79
2014	87.34	2003	73.92
2015	75.72	2004	47.82
2016	52.65	2005	64.80
2017	82.13	2006	54.03
2018	35.75	2007	72.30
		2008	105.39
		2009	54.68
		2010	77.00
		2011	84.53
		2012	49.55
		2013	43.92
		2014	82.32
		2015	82.05
		2016	81.69
		2017	71.88
		2018	45.50